CENTER FOR ASTROPHYSICS
HARVARD & SMITHSONIAN

Submillimeter Array Newsletter

Number 38, July 2024

CONTENTS

FROM THE DIRECTOR

Dear SMA Newsletter readers,

The SMA continues to support a significant oversubscription rate of observations. Scientists within and outside the CfA are publishing exciting papers. In this Newsletter, you will have a chance to read of the SMA being used for interferometric imaging of molecular line emission from the young planetary nebula NGC 3132, demonstrating its value as an essential complement to infrared observations from JWST; also of the SMA's detection of an extreme millimeter flare from the young class III star, and an intriguing description of the SMA's use to characterize a newly detected, enormous planet-forming disk.

SMA staffing has had two important additions this past year. John Miller is our new IT Specialist working in Hawaii, and Nick Smith fills out our Telescope Operator staffing to five. We are reaping the benefits of both of these additions already with John upgrading and replacing failing data storage systems, and Nick enabling full coverage of Hawaii observing shifts.

The administrative staff was short handed following the departure of two key members last year. Since then, Pamela Nehls has stepped up to a more significant administrative role in Hawaii, while Elizabeth Shepard covers Cambridge, Massachusetts, in addition to her role as the Radio and Geoastronomy Division Administrator, with temporary support from Ashley Spears.

Telescope maintenance challenges persist, as we've known they would. We all anxiously anticipate the arrival of new wSMA cryostats and receivers to alleviate the ongoing issues with the aging cryogenic systems of the current receiver sets. In the meantime, staff continue their exhaustive efforts to keep the SMA in operation while upgrade activities are going on simultaneously. Displacers have been returned to Sumitomo for repair, the elevation drive motor for Antenna 7 has been returned to Integrated Magnetics for re-assembly, tachometers have been returned to Cambridge for diagnostics, and the Maser is being prepared for shipment back to T4 Science thanks to Jonathan Weintroub's successful pursuit of a supplement to an MIT-Haystack NSF grant. Telescope upgrade activity is advancing as we anticipate the first set of new generation motor drive electronics from Glentek next month. A new chopper drive system is also progressing toward an end-of-summer shipment to Hawaii for installation and testing. Technical developments continue for the wSMA, including a novel optical diplexer described in this issue.

The Smithsonian continues to make significant investments in the SMA infrastructure. In this issue, Clint Monceaux reports on facility projects including the Hilo Backup Generator, the Active Power System for summit, and the Packaged Air Conditioning Unit (PACU).

Please read our news on recent community outreach from Pamela Nehls, our newly appointed Education and Engagement Outreach Coordinator.

Tim Norton

SMA REVEALS THE MOLECULAR EXOSKELETON OF THE SOUTHERN RING NEBULA

Joel H. Kastner[1], David Wilner[2], Paula Moraga Baez[1], Jesse Bublitz[3], Orsola De Marco[4], Raghvendra Sahai[5], Al Wootten[6]

Planetary nebulae are fleetingly brief but highly revealing episodes that mark the termination of the lives of intermediate-mass (1-8 solar mass) stars. Late in the asymptotic giant branch (AGB) evolutionary stages of such a star, H and He shell burning around the star's inert, contracting C-O core generates luminosities on the order of 10^4 Lsun, and the star's cool, extended (~1 au radius) envelope becomes rich in dust and molecular gas. This tenuously bound stellar envelope is ripe for ejection via the combination of Mira-like (long-period) stellar pulsations and radiation pressure on dust (Hofner & Olofsson 2018, and references therein). Indeed, the dustiest (most highly obscured) AGB stars are observed to lose mass at rates of 10^{-7} to 10^{-4} Msun/yr at outflow velocities of 10-20 km/s; the latter is – not coincidentally – roughly the escape velocity at 1 au from a solar-mass star. As the AGB stellar envelope is stripped, the hot AGB stellar core becomes exposed, and the star traverses the HR diagram horizontally, from effective temperatures of ~3,000 K to ~10^5 K, on timescales <~1000 yr. Once its effective temperature exceeds 3 x 10^4 K, the former AGB star develops an intense UV radiation field that begins to ionize the ejected AGB envelope, forming a planetary nebula (PN). The resulting ionized, ~10^4 K PN is characterized by H and He recombination lines and forbidden lines of metals (Kwitter & Henry 2022). The escape velocity from the (newly compact) stellar photosphere ramps up to ~1000-2000 km/s, setting the stage for shock-producing wind collisions that can result in ~10^6 K, X-ray-emitting plasma within the PN (Kastner et al. 2012, and references therein).

Under the foregoing formation scenario, PNe should appear as spherical, photoionized nebulae that are bounded by neutral (fossil) AGB ejecta, possibly displaying sharp rims where the central star's fast wind has swept up this previously ejected AGB envelope material. However, decades of high-resolution ground-based and HST imaging have established that most planetary nebulae are in fact highly structured, heterogeneous objects (e.g., Sahai & Trauger 1998; Balick et al. 2023). PN morphologies are often axisymmetric (bipolar) or point-symmetric, and it is not uncommon to observe multiple axes of symmetry in the same object. Various hypotheses have been put forward over the years to explain these sharp departures from spherical symmetry, including magnetic fields, stellar activity, and the influence of binary companions (Balick & Frank 2002, and references therein). Given the commonality of close binaries among field main-sequence stars, and the significant wind-redirecting angular momentum reservoir and gravitational potential energy represented by a close binary companion, the prevailing (but by no means unanimous) contemporary view is that this last (binary progenitor star) shaping mechanism is most likely responsible for the array of PN morphologies and, in particular, for generating axisymmetric nebulae (De Marco 2009; Jones & Boffin 2017).

Furthermore, there is a direct correlation between the appearance of axisymmetric structures in PNe and the presence of significant masses of molecular gas and dust in the nebulae. Indeed, detections of bright near-IR H_2 emission and mm-wave CO emission from hot and cold molecular gas (respectively) in a PN almost guarantees that the nebula is bipolar or Ring-like in structure, with its overdense equatorial regions providing the main molecular gas reservoir (Kastner

[1]Rochester Institute of Technology, [2]Center for Astrophysics | Harvard & Smithsonian,[3]Green Bank Observatory,[4]Macquarie University,[5]NASA/JPL,[6]NRAO

Figure 1: Color JWST image overlays of emission from H recombination lines and [S III] (left panel) and multiple transitions of H_2 (right panel), adapted from De Marco et al. (2022) and an associated STScI press release[1]. The field of view of each image is ~120"x120"; N is up and E to the left. Note the clean separation of the nebula into relatively smooth, compact ionized gas vs. highly structured, extended molecular gas components in the left and right panels (respectively). The bright star just to the left of the geometric center of the nebula is a wide (~1000 au) separation companion to the optically fainter progenitor star. The red appearance of the PN progenitor in the left panel is due to its large thermal mid-IR excess, indicative of a dusty disk.

et al. 1996; Huggins et al. 2005). Assuming this molecular gas represents fossil AGB ejecta, then the implication is that the progenitor star's mass loss was already proceeding in axisymmetric fashion prior to the onset of photoionization and the central star's fast, post-AGB wind (e.g., Balick et al 2019). The combination of bipolar structure and large residual molecular gas masses in PN also appears to be a marker of higher-mass (>~2 solar mass) PN progenitor stars (Kastner et al. 1996 and refs. therein).

The PN NGC 3132 (the "Eight-burst" nebula, aka the Southern Ring) is a prime example of such a molecule-rich, Ring-like PN. The nebula has been the subject of scrutiny for more than a century (Campbell & Moore 1918; Shapley & Paraskevopoulos 1940; Evans & Thackeray 1950), and was among the first PNe mapped in mm-wave CO (Sahai et al. 1990) and imaged in near-IR H_2 (Kastner et al. 1996). JWST has now made NGC 3132 a "coffee-table" celestial object, via its inclusion among the handful of targets of JWST Early Release Observations (EROs). As demonstrated by De Marco et al. (2022), the JWST ERO NIRCam and MIRI images, which cover the wavelength range ~1-18 microns, cleanly dissect NGC 3132 into ionized and molecular gas components (Fig. 1). The JWST images furthermore yielded strong if indirect evidence for at least one and possibly two interacting companions to the PN progenitor star, in the form of an IR excess at the central star that is indicative of a long-lived dusty disk around the progenitor (Fig. 1, left panel), and interrupted concentric ring structures in the nebula's extended, highly structured H_2 halo (Fig. 1, right panel).

While the JWST ERO images revealed the H_2 emission morphology of NGC 3132 in unprecedented detail, the JWST narrow-band imaging cannot be used to infer the 3D structure of the PN's expanding molecular envelope; moreover, IR H_2 imaging is only sensitive to "hot" (~1000 K), UV- and/or shock-excited molecular gas. Observations of mm-wave CO emission are necessary to probe the colder (~30-100 K) gas that represents the bulk of the mass of the molecular envelope, and to trace the molecular gas kinematics. But previous to the JWST ERO imaging, NGC 3132 had only once been the subject of mm-wave CO mapping observations — more than three decades ago, and only at a limited number of pointings with the 20" diameter beam of the late SEST 15-meter telescope (Sahai et al. 1990).

Clearly, the time was ripe for mm-wave interferometric imaging of molecular line emission from NGC 3132. Hence, in May

[1]J. DePasquale (STScI); https://webbtelescope.org/contents/news-releases/2022/news-2022-059

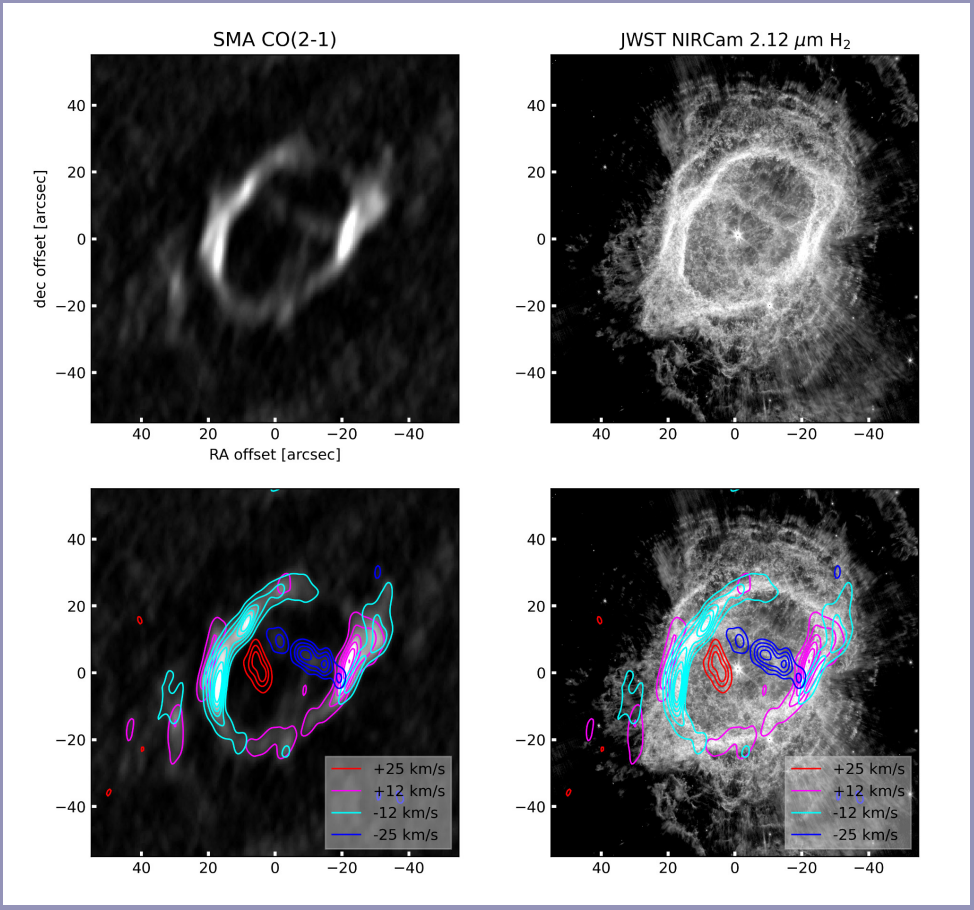

Figure 2: Comparison of JWST/NIRCam and SMA imaging of NGC 3132. ***Top left:*** velocity-integrated (moment 0) SMA ^{12}CO(2–1) image. ***Top right:*** JWST/NIRCam 2.12 micron H_2 image. ***Bottom left:*** contours of ^{12}CO(2–1) emission integrated over selected velocity ranges overlaid on the ^{12}CO(2–1) moment 0 image. The (four) velocity ranges are labeled with their central velocities with respect to systematic (i.e., -25, -12, +12, and +25 km/s). ***Bottom right:*** the same sets of velocity-resolved ^{12}CO(2–1) emission contours overlaid on the JWST/NIRCam H_2 image. Figure adapted from K24.

2023, we obtained a small mosaic of Submillimeter Array (SMA) pointings targeting NGC 3132, at ~5" spatial resolution, in the 1.3 mm window (Kastner et al. 2024; hereafter K24). Our spectrometer settings provided coverage of the J=2-1 transitions of CO and isotopologues and the N=2-1 hyperfine complexes of CN at ~1 km/s velocity resolution. These observations yielded high-quality maps of ^{12}CO(2-1) and CN(2-1), a somewhat noisier map of ^{13}CO(2-1), and nondetections of C^{18}O(2-1) and 1.3 mm continuum emission.

The results of the SMA ^{12}CO(2-1) mapping, including a comparison with JWST/NIRCam H_2 imaging, are summarized in Fig. 2. The morphology of the velocity-integrated (moment 0) SMA ^{12}CO(2-1) image is observed to closely trace that of the near-IR H_2 emission, with the brightest emission found along the minor axis of the main, elliptical (~50"x35") ring of NGC 3132. The SMA ^{12}CO(2-1) data further reveal various new, fundamental aspects of the velocity field of the molecular gas. In particular, Fig. 2 demonstrates that the east limb of the main, bright ring (hereafter Ring 1) is observed to be primarily blueshifted, and the west limb primarily redshifted, with respect to the systemic velocity of NGC 3132. This velocity gradient indicates that Ring 1 is oriented with its eastern (western) side toward (away from) the observer, although the presence of weaker, spatially offset redshifted and blueshifted components along the east and west limbs of Ring 1 (respectively) suggests a relatively small tilt out of the plane of the sky. Also notable are the high-velocity (redshifted and blueshifted) CO knots, with filamentary H_2 counterparts, that are seen projected within Ring 1.

The left panels of Fig. 3, which display the SMA ^{12}CO(2-1) data cube "collapsed" along each of its three dimensions, clearly illustrate that Ring 1 is indeed a tilted molecular ring. Ring 1 thus likely traces the dense equatorial plane of NGC 3132. This expanding, molecule-rich toroidal structure is closely analogous to the expanding molecular tori observed in pinched-waist, bipolar PNe (e.g., NGC 6302; Santander-Garcia et al. 2017); but in the case of NGC 3132, as for other Ring-like PNe (Kastner et al. 1994), the molecular torus is viewed at low inclination.

The position-velocity images in the middle left and bottom left panels of Fig. 3 furthermore reveal that the high-velocity CO features seen projected within Ring 1 in Fig. 2 are in fact the brighter regions of a second expanding ring of molecular gas — and that this second ring (hereafter Ring 2) is oriented nearly edge-on to the line of sight, i.e., nearly perpendicular to

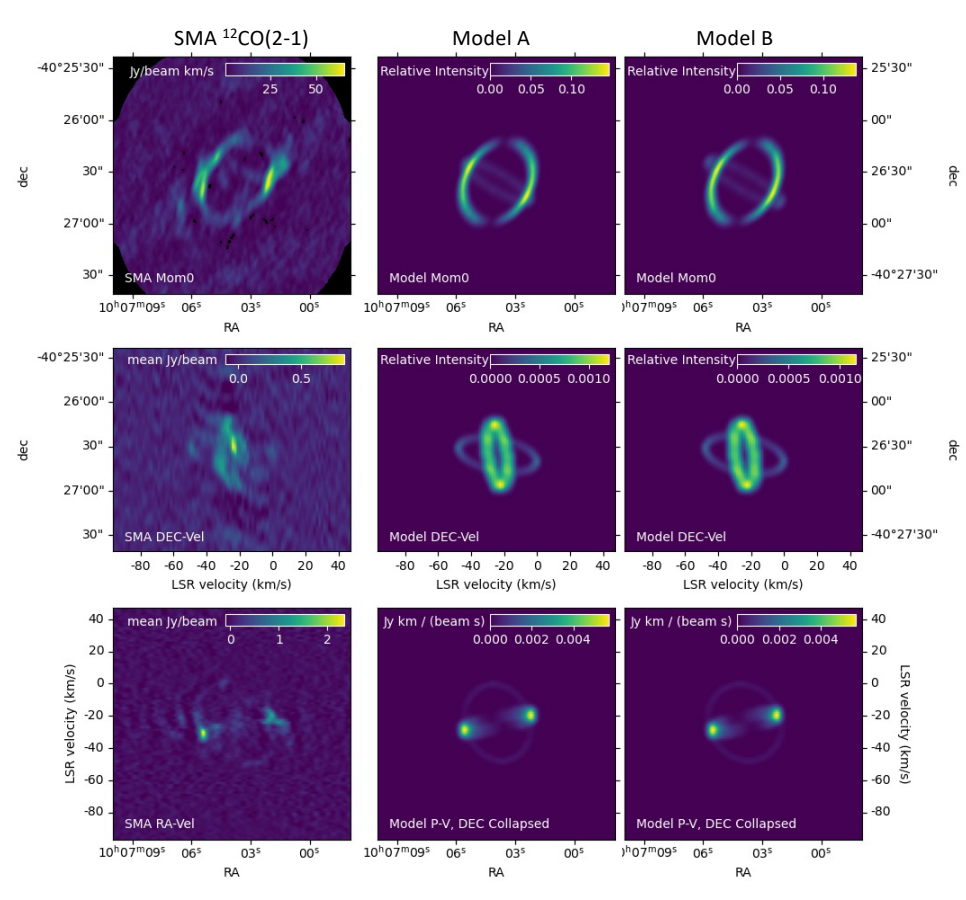

Figure 3: Left panels: three views of the SMA ^{12}CO(2–1) data cube obtained for NGC 3132. **Top left frame:** the noise- clipped moment 0 image. **Middle left** and **bottom left frames:** position-velocity images obtained by collapsing the data cube along the RA and decl. axes, respectively. **Middle and right columns:** the equivalent views of two alternative, simple geometrical models for the two-ring structure of NGC 3132's expanding molecular envelope (see text). Figure adapted from K24.

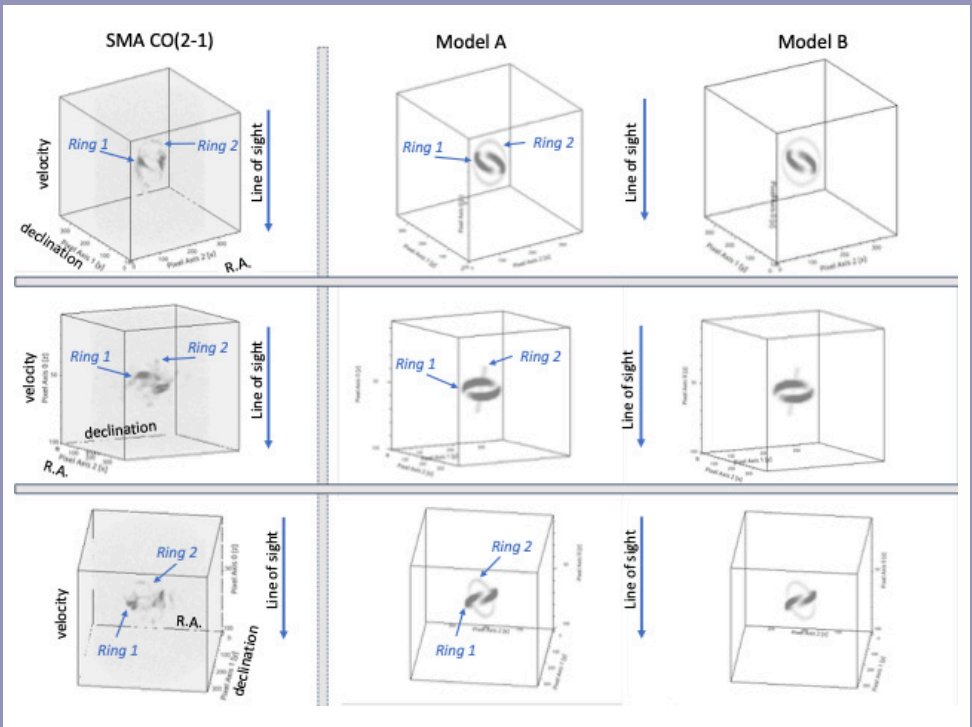

Figure 4: Left panels: three example volume renderings of the SMA ^{12}CO(2–1) data cube, with R.A., decl., and velocity as the x-axis, y-axis, and z-axis (respectively). The dimensions of the cube are ~180" along the R.A., decl. (x, y) axes and -96 to +46 km/s along the velocity (z) axis. **Middle panels:** the corresponding views of Model A. **Right panels:** the corresponding views of Model B. Figure adapted from K24.

Ring 1. This two-ring structure is also apparent in the volume renderings of the data cube displayed in the left-hand panels of Fig. 4.

Motivated by the structures observed in the SMA ^{12}CO(2-1) data in the moment 0 and P-V images and data cube volume renderings, we constructed simple geometric models of NGC 3132's molecular emitting region. The basic model consists of two rings whose inclinations, expansion velocities, dynamical ages, and ellipticities are adjustable parameters. Experimentation established that two alternative realizations of this basic model provide equally convincing representations of the data (see middle and right columns of Figs. 3 and 4). In the first (Model A), the two rings are assumed to have identical expansion velocities (25 km/s) and dynamical ages (3700 yr), and are oriented nearly orthogonal to each other, with Ring 1 viewed at low (15 degree) inclination and Ring 2 viewed within 15 degrees of edge-on. In this model, Ring 1's ellipticity in the moment 0 image is the result of intrinsic ellipticity (major/minor axis ratio of ~1.25), as opposed to viewing angle. In the second model (Model B), both rings are assumed circular; this requirement imposes an inclination of ~45 degrees on Ring 1 (such that its orientation relative to Ring 2 is ~60 degrees) and, even more significantly, requires the two rings to have sharply contrasting dynamical ages (9250 yr and 3700, respectively) and expansion velocities (10 km/s and 25 km/s). If one adopts Model A, one implication is that the molecule-rich envelope of the AGB progenitor of NGC 3132 was ejected in a single, short-lived episode that terminated its AGB evolution. Future multi-epoch JWST imaging of NGC 3132 will readily distinguish between these (degenerate) model parameter sets, by establishing the plane-of-sky expansion velocity and (hence) dynamical age of Ring 1.

These new SMA observations of NGC 3132 have reinforced the connections between the mass and distribution of molecular gas in a PN, its intrinsic (bipolar) structure, and the mass of the PN progenitor star. With regard to this last aspect, K24 show that the SMA-measured (integrated) ^{12}CO: ^{13}CO and CN: ^{12}CO line ratios are consistent with De Marco et al. (2022)'s conclusion that the PN is derived from a ~3 solar mass progenitor. On the other hand, as discussed in K24, the presence of two, nearly orthogonal rings of molecular gas within NGC 3132 is difficult to reconcile with models invoking interacting binary systems as PN shaping agents. We speculate that the ejected molecular envelope may initially have been ellipsoidal, with a profound equatorial density enhancement (Ring 1), and that the polar regions were subsequently perforated by a series of misaligned, jet-like outflows, leaving behind Ring 2 and generating a bipolar or perhaps multipolar PN. Such a "misaligned jet" scenario, which is also a common feature of bipolar/multipolar PNe (e.g., Balick et al. 2023), would likely require an interacting tertiary component in the NGC 3132 progenitor system (as proposed by De Marco et al. 2022).

These results from SMA molecular-line mapping observations of NGC 3132 should serve as motivation for future SMA observations of additional nearby, molecule-rich PNe. The SMA's ability to elucidate a PN's detailed, 3D molecular gas distribution and dynamics serves as an essential complement to high-resolution JWST imaging of H_2 in such objects, providing unique insight into the death throes of intermediate-mass stars with close companions.

REFERENCES

- Balick, B., & Frank, A. 2002, ARA&A, 40, 439
- Balick, B., et al. 2019, ApJ, 877, 30
- Balick, B., et al. 2023, ApJ, 957, 54
- Campbell, W.W., & Moore, J.H. 1918, Publ. Lick Obs., 13, 75
- De Marco, O. 2009, PASP, 121, 316
- De Marco, O., et al. 2022, Nature Astronomy, 6, 1421
- Evans, D.S., & Thackeray, A.D. 1950, MNRAS, 110, 429
- Hofner, S., & Oloffson, H. 2018, A&ARv, 26, 1
- Huggins, P., et al. 2005, ApJS, 160, 272
- Jones, D., & Boffin, H.M.J. 2017, Nature Astronomy, 1, 117
- Kastner, J.H., et al. 1994, ApJ, 421, 600
- Kastner, J.H., et al. 1996, ApJ, 462, 777
- Kastner, J.H., et al. 2012, AJ, 144, 58
- Kastner, J.H., et al. 2024, ApJ, 965, 21 (K24)
- Kwitter, K.B., & Henry, R.B.C. 2022, PASP, 134:022001
- Sahai, R., et al. 1990, A&A, 234, L1
- Sahai, R., & Trauger, J.T. 1998, 116, 1357
- Santander-Garcia, M., et al. 2017, A&A, 597, A27
- Shapley, H., & Paraskevopoulos, J.S. 1940, PNAS, 26, 31

A GIANT COSMIC BUTTERFLY FLUTTERS INTO VIEW

Kristina Monsch[1], Joshua Bennett Lovell[1], Ciprian T. Berghea[2], Gordian Edenhofer[1,3,4], Garrett K. Keating[1], Sean M. Andrews[1], Ammar Bayyari[5], Jeremy J. Drake[1,6], David Wilner[1]

The Submillimeter Array (SMA) has revealed the nature of a newly detected, enormous planet-forming disk, which appears like a giant, cosmic butterfly in the night sky. This discovery offers new insight into the environments where planets form. Officially known as IRAS 23077+6707 (IRAS 23077, for short), this giant planet-forming disk is about 1000 light-years from Earth. IRAS 23077 was initially discovered in 2016 by Ciprian T. Berghea from the US Naval Observatory using the Panoramic Survey Telescope and Rapid Response System (Pan-STARRS) and was reported only recently in the scientific literature. In a second paper, published in *The Astrophysical Journal Letters* in May 2024, and which was covered internationally by various media outlets (see e.g. the *BBC Sky & Night Magazine*, *The Associated Press News* or *The Washington Post*), SMA DDT observations obtained in spring 2023 (2022B-S054, PI: K. Monsch) provide compelling evidence that IRAS 23077 is the largest planet-forming disk in the sky, with dust and carbon monoxide (CO) gas extents of at least 12''–14'', and CO in Keplerian rotation. IRAS 23077 has no reported distance estimate, but since it is located in the Cepheus star-forming region (180-800 pc), its disk likely spans thousands of au in radius.

Planet-forming, or so-called "protoplanetary" disks are rotating accumulations of gas and dust surrounding young stars and are the birthplaces of planets, moons, and smaller bodies that make up planetary systems. By studying protoplanetary disks,

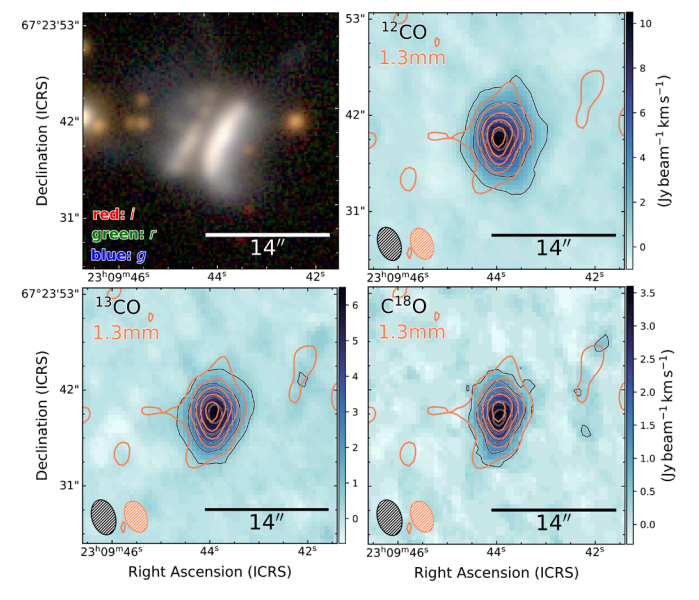

Figure 1: Comparison of optical scattered-light and (sub)millimeter emission of IRAS 23077. **Top left:** RGB-composite image, showing the optical scattered-light emission as seen by Pan-STARRS. **Top right:** SMA ^{12}CO integrated intensity (or "moment 0") map, overlaid with its respective contours, as well as the 1.3 mm continuum contours, drawn at the 10%, 30%, 50%, 70%, and 90% levels of their corresponding maximum emission. **Bottom left:** same for ^{13}CO. **Bottom right:** same for C^{18}O. In the lower right of each panel 14'' scale bars are shown, while the effective CO (black) and continuum (orange) beams are shown in the lower left of the SMA images.

[1]Center for Astrophysics | Harvard & Smithsonian; [2]U.S. Naval Observatory (USNO); [3]Max Planck Institute for Astrophysics; [4]Ludwig Maximilian University of Munich; [5]Department of Physics and Astronomy, University of Hawaii; [6]Lockheed Martin

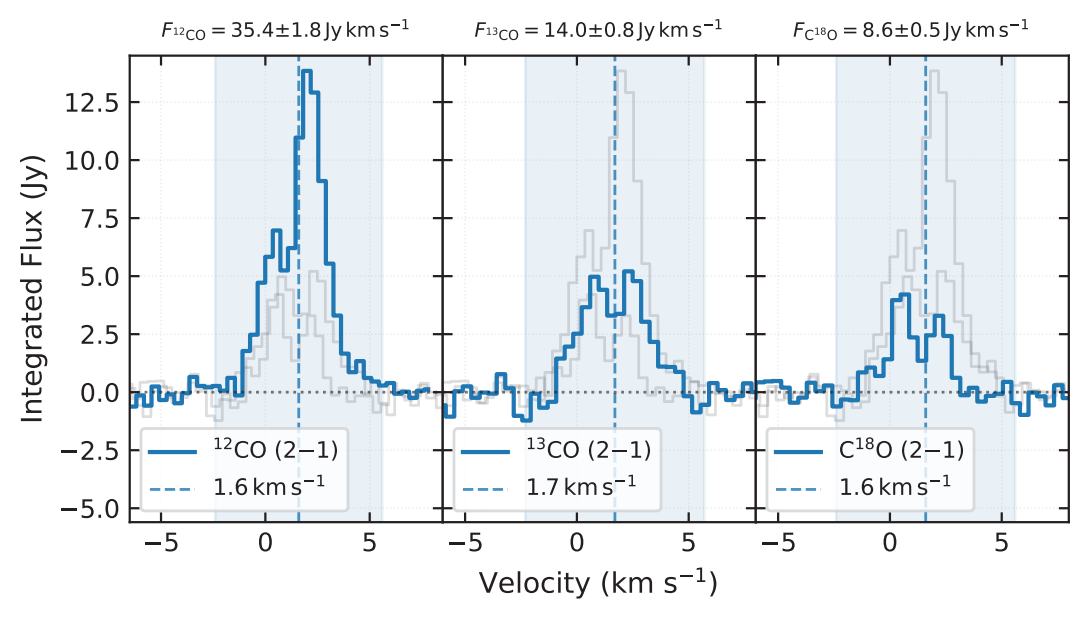

Figure 2: Line spectra of the ^{12}CO, ^{13}CO, and C^{18}O J = 2–1 lines with their respective centroid velocities. The double-peaked line profiles confirm that the CO gas must be in Keplerian rotation around its central star.

we can gain critical insights into the processes of planet formation, the conditions that lead to the development of planetary systems, and the chemical and physical environments of early star systems (see Williams & Cieza 2011; Andrews 2020, for reviews). Investigations into these disks help us understand the diversity of exoplanetary systems, the potential for habitability, and the origins of our own solar system.

Some planet-forming disks like IRAS 23077 are viewed 'edge–on', meaning they are oriented such that their own dust and gas–rich disks entirely obscure the light emitted from their parent star. This makes them inherently faint at optical and near-infrared wavelengths and thus hard to detect. The recent work of Angelo et al. (2023) confirms that the number count of edge-on disks falls far short of simulated disk populations in the Galaxy and that there may be many more such edge-on disks awaiting discovery. In contrast to more typical edge-on disks, IRAS 23077 is exceptionally bright at optical and infrared wavelengths, which aided its serendipitous discovery in the Pan-STARRS data.

The combination of scattered-light imaging with interferometric observations in the millimeter regime has proven to be especially successful in characterizing edge-on disks in detail (see e.g., Wolf et al. 2003; Bujarrabal et al. 2008, 2009; Sauter et al. 2009; Wolff et al. 2021), as both types of observations trace different regions of a system and thus unique physical processes. On one hand, (sub)millimeter observations are sensitive to the longer wavelength radiation being reemitted from larger (millimeter- to centimeter-sized) dust grains close to the disk midplane and thus typically appear in extended line (or "needle-like") morphologies. On the other hand, optical and near-infrared observations trace smaller, micron-sized dust grains in the hotter, outer envelope and the disk surface layers that scatter the light of the central star and thus create two bright, highly flared lobes.

IRAS 23077 shows the typical morphological features of an edge-on protoplanetary disk, namely two elongated bright reflection nebulae (tracing the upper and thus hotter layers of the disk atmosphere), separated by a dark lane (tracing the disk midplane) that obscures the light emitted by the central star (see the first panel of Figure 1). Notably, IRAS 23077 also shows two faint filaments extending northwards by almost 9'', which likely trace the arcs of the disk's flared upper layers.

While their stars may be shrouded, the dust and gas signatures of edge-on protoplanetary disks can still be exceptionally bright at millimeter wavelengths. The top right and bottom panels of Figure 1 show the integrated intensity (or "moment 0") maps for the CO emission lines. All three gas lines are clearly detected, with disk emission (detected at >3σ level) covering more than 14'' for both ^{12}CO and ^{13}CO and 12'' for C^{18}O (i.e., three to four beams across the radial disk extent). Notably, while being significantly less abundant than ^{12}CO, the extents of both the ^{13}CO and C^{18}O emissions along the radial and vertical directions are comparable to the ^{12}CO emission, revealing this as a highly gas-rich system.

As expected for disks in Keplerian rotation, the line profiles for all three CO isotopologues as shown in Figure 2 are double peaked, with velocity centroids of 1.6, 1.7, and 1.6 km/s respectively. Out of these, the ^{12}CO line profile is observed as asymmetric, with its redshifted (western) component being

around 2 times brighter than its blueshifted (eastern) component, which is likely a consequence of the ^{12}CO emission being optically thick, preventing us from observing as much CO on the disk rear side.

IRAS 23077 exhibits three prominent asymmetries in the optical scattered light emission. First, its western lobe is brighter than its eastern lobe by a factor of 6, typical for disks with sky-projected inclinations that are not perfectly edge-on (due to preferential grain scattering). Second, in the eastern (fainter) lobe, the southern region is brighter than the northern one by a factor of 3, whereas in the western (brighter) lobe, the northern and southern region brightnesses are within 1%. Lateral asymmetries can be a result of foreground extinction preferentially dimming the northeast of the disk. However, they could also imply a misaligned, inner disk or a warp that would cast shadows on the observed disk. A suite of higher-resolution observations using the SMA at extended and very extended configurations have been recently approved (PI: Joshua B. Lovell), and will allow us to derive the origin of the observed brightness asymmetries in IRAS 23077.

REFERENCES

- Andrews, S. M., Liu, M. C., Williams, J. P., & Allers, K. N. 2008, ApJ, 685, 1039
- Angelo, I., Duchene, G., Stapelfeldt, K., et al. 2023, ApJ, 945, 130
- Berghea, C.T., Bayyari, A., Sitko, M.L., et al. 2024, ApJL, 967, L3
- Bujarrabal, V., Young, K., & Fong, D. 2008, A&A, 483, 839
- Bujarrabal, V., Young, K., & Castro-Carrizo, A. 2009, A&A, 500, 1077
- Ho P. T. P., Moran J. M. and Lo K. Y. 2004, ApJL, 616 L1
- Monsch, K., Lovell, J.B., Berghea, C.T., et al. 2024, ApJL, 967, L2
- Sauter, J., Wolf, S., Launhardt, R., et al. 2009, A&A, 505, 1167
- Williams, J. P., & Cieza, L. A. 2011, ARA&A, 49, 67
- Wolf, S., Padgett, D. L., & Stapelfeldt, K.R. 2003, ApJ, 588, 373
- Wolff, S.G., Duchene, G., Stapelfeldt, K.R., et al. 2021, AJ, 161, 238

SMA DETECTION OF AN EXTREME MILLIMETER FLARE FROM THE YOUNG CLASS III STAR HD 283572

Joshua Bennett Lovell[1], Garrett K. Keating[1], David J. Wilner[1], Sean M. Andrews[1], Meredith MacGregor[2], Ramisa Akther Rahman[1,3], Ram Rao[1], Jonathan P. Williams[4]

Stellar flares are extreme radiation outbursts from the surfaces of stars, analogous to solar flares commonly observed on the Sun, whereby stored magnetic energy accelerates charged particles through surrounding stellar plasma, radiating brightly across the electromagnetic spectrum (Dulk 1985, Fiegelson et al. 1999, Güdel 2002, Fletcher et al. 2011, Candelerasi et al. 2014). At millimeter wavelengths, stellar variability campaigns hunting for flaring activity have mostly targeted nearby main sequence M-type stars, such as Proxima Centauri and AU Mic, finding extreme flaring events on timescales of 1-10 seconds (see e.g., MacGregor et al. 2020, 2021, Howard et al. 2023). A handful of millimeter flares have also been detected from the closest Sun-like star, ε Eridani (eps Eri; Burton et al. 2022), and a range of other M and K-type stars from millimeter survey telescopes (e.g, the South Pole Telescope and the Atacama Cosmology Telescope, see e.g., Guns et al. 2021, Naess et al. 2021).

Stellar flaring rates decline with age due to stellar spin-down (Davenport et al. 2019). Decades of monitoring at radio and X-ray wavelengths have shown that young T-Tauri stars are highly active in comparison to older main sequence stars. Whilst active, stars can undergo intense periods of flaring (Favata et al. 1998, Stelzer et al. 2007, Dzib et al. 2015, Forbrich et al. 2017, Vargas-González et al. 2021). The intensity of a stellar flare has to be especially high for these to be visible at millimeter wavelengths, and as such only a small number of flares from T-Tauri stars have been confirmed (see e.g., Massi et al. 2002, 2006, 2008, Bower et al. 2003, Salter et al,. 2010, Mairs et al. 2019). Only recently are the statistics of millimeter stellar variability coming to light (e.g., such as from studies of the ~Myr-old Orion Nebula Cluster (ONC) and JCMT Gould-Belt transient surveys; Vargas-González et al. 2023, Johnstone et al. 2022 respectively). Whilst millimeter flares have likewise been observed from a handful of classical RS CVn (main sequence) binaries (Beasley & Bastian 1998, Brown & Brown 2006), millimeter flares appear to be rarer than in X-ray or radio wavelengths, and also much stronger for younger versus main sequence stars.

As part of a survey of young stellar objects (YSOs) at the 'class III' stage of evolution (stars lacking much-if-any mid–infrared dust excesses), a recent SMA study reported the detection of an extreme millimeter brightening event associated with HD 283572 (Lovell et al. 2024; Fig. 1). Considering all available data such as the timespan of the event (spanning at least 9 hours), its negative spectral slope, linear polarization fraction, the team interpreted the sudden brightening as due to a powerful stellar flare, amongst only a handful of events from class III YSOs, and amongst the most powerful millimeter stellar flares ever reported in the literature. HD 283572 is currently a mid–G type star, with a Solar–like effective temperature, and a mass of about 1.4 solar masses, suggesting that it will form a late–A type star when it reaches the main sequence. A–type stars are typically inactive on the main sequence lacking a dynamo, however this study demonstrates that these too can be active flare sources at early stages of their lives.

Although HD 283572 was observed on 8 separate nights, including 5 via an SMA DDT, the event in question happened on January 17th 2022 (track `T3') and no other millimeter flares were detected from HD 283572 either prior to nor since.

[1]Center for Astrophysics | Harvard & Smithsonian, [2]Department of Physics and Astronomy, Johns Hopkins University, [3]William & Mary College, [4]Institute for Astronomy, University of Hawai'i at Mānoa

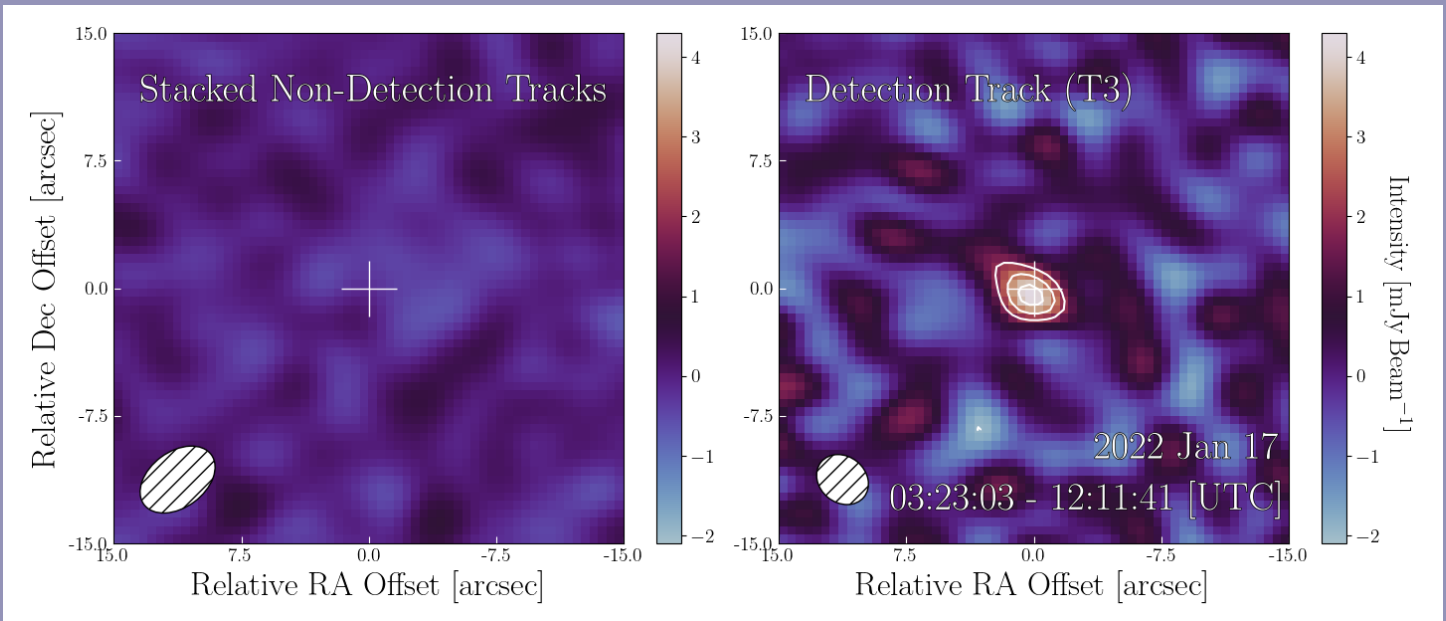

Figure 1: Left: cleaned image of the combined SMA measurement sets from all tracks in which no significant emission is detected. **Right:** cleaned image of the SMA measurement set for track `T3', in which a significant point source is present at the location of HD~283572. The noise is lower in the image with no detection (rms 0.24 mJy/beam) than the image with the detection (rms 0.48 mJy/beam). Contours are at +/-4, 6 and 8 times the rms noise levels. SMA beams are in the lower left corners.

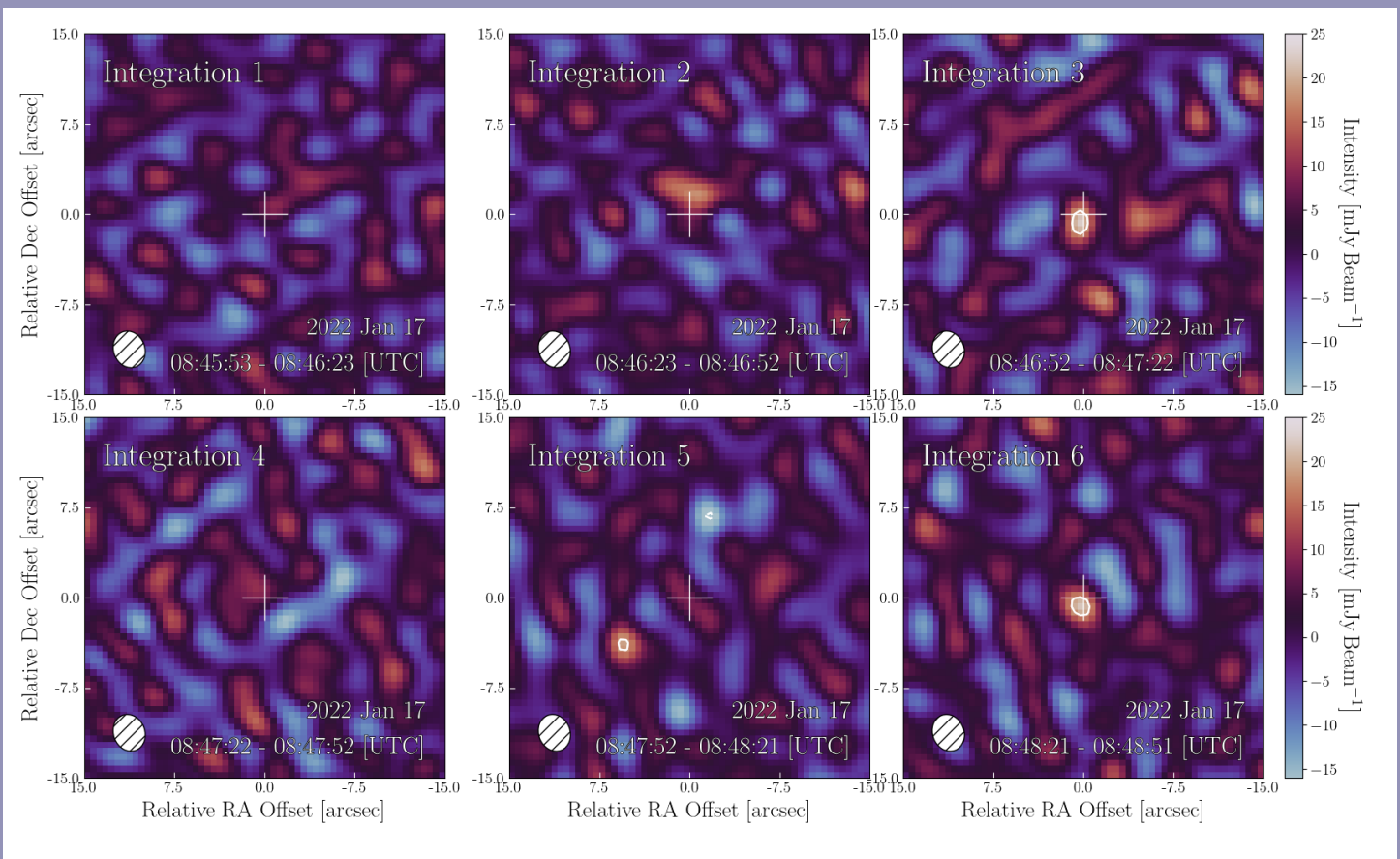

Figure 2: From left–right, then top–bottom: maps of the 30 second integrations during the flare Track T3, segment 13 (T3:S13; when the event F1 was detected). Image rms values range from 3.8-4.8 mJy/beam. Integrations 3 and 6 show emission at the 23 mJy and 25 mJy level respectively, coincident with HD 283572's location. Contours are at +/-4 times the rms levels. SMA beams are in the lower left corners.

When stacked, the non–detections of the 7 nights combined suggest the star is normally in an inactive state, with a total flux <0.72mJy (3σ). In contrast, the peak brightness that the team reported from their 17 Jan 2022 data saw the star emit ~25mJy in a single 30 second window, an enhancement versus the inactive level of at least 100 times (Fig. 2). Moreover, given the 9 hour nature of the event and the star's ~125 pc distance, compared to nearby millimeter flares from e.g., eps Eri, HD 283572's flare was over 1000 times more luminous, and over 1000 times longer, i.e., >1,000,000 times more energetic.

Connecting the emission properties of the flare to those of the star yields interesting findings about the stellar environment. Firstly, the spectral slope points towards either gyro-/synchrotron emission being the mechanism responsible (with perhaps synchrotron favored given the limit on the linear polarization fraction). In the synchrotron case, the team estimated the stellar magnetic field strength at the level of <1 kG, whereas if the emission came from gyro-synchrotron, the field strength is a much higher >9 kG. In either case, these results demonstrate the possibility of studying stellar magnetic fields from transient millimeter flaring events. The team corroborated their findings by investigating the star's radio properties (from the 2–4GHz VLA sky survey) likewise finding the data to be highly variable (Fig. 3).

The underlying cause of the flare however remains unknown. The team posited that the event could have been purely stochastic (e.g., comparable to typical Solar flares despite the difference in their observed millimeter properties) or instead triggered via stellar magnetospheric interactions with an unknown/unseen low–mass companion (happening periodically within the binary orbital cycle, as seen to occur for early stage YSOs (e.g., V773 Tau and DQ Tau; Massi et al. 2006, Salter et al. 2010) and main sequence RS CVn binaries (e.g., sigma Gem; Brown & Brown 2006)). The latter case appears more likely given the timescale, strength, and spectral slope of HD 283572's flare, which appears to better match these binary–driven events. Yet, due to HD 283572's very large rotational velocity, data does not currently exist to search for the presence of a low–mass companion and corroborate this hypothesis.

The work of Lovell et al. 2024 suggests that temporal analyses of class III YSO millimeter observations are generally warranted to distinguish between stellar and circumstellar components. Importantly, class III stars open a window on planet formation/disk evolution after the dispersal of the bulk protoplanetary/ primordial disk material. Class III YSOs can retain large reservoirs of cold dust, and/or smaller reservoirs of hot dust that trace ongoing terrestrial planet formation processes (Lovell et al. 2021; Michel et al. 2021) over timescales that fully span pre-main sequence evolution (Kenyon & Bromley 2004; Morbidelli et al. 2012). Combined with the implication that proton-rich flare events can disrupt the growth of planetary atmospheres (Tilley et al. 2019), constraints on the physics of class III YSO flares could provide key inputs to exoplanet atmospher-

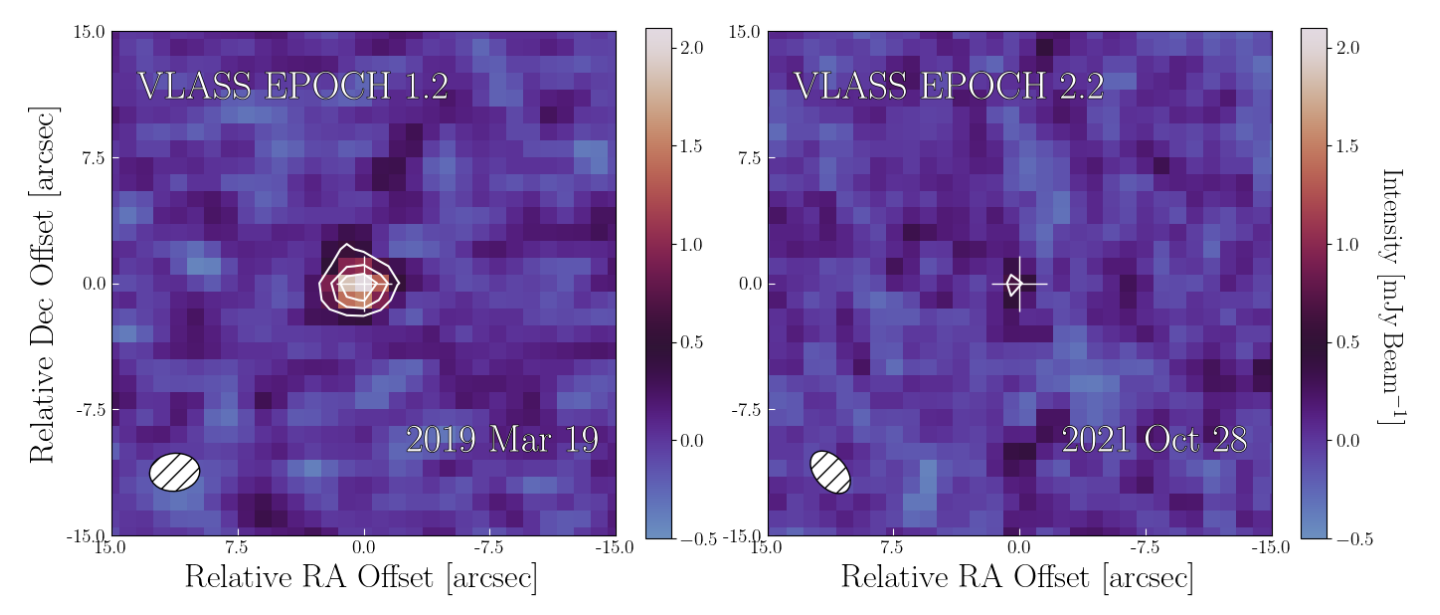

Figure 3: VLASS `Quick Look' images (**left:** epoch 1.2; **right:** epoch 2.2). In both images, the coordinates are centered on the location of HD 283572. Clear in 1.2 is the detection of a bright point source, whereas in 2.2 the detection significance is much reduced. The rms in both images is 0.125 mJy/beam. Contours are at +/-4, 8 and 12 times the rms noise levels. VLA beams are in the lower-left corners.

ic growth models. This work further highlights the power of the SMA's wide bandwidth and SWARM rapid–scan capabilities to enable a stellar variability study covering timescales from hours down to just 5 seconds, spanning observations over baselines of over one year.

REFERENCES

- Beasley, A. J., & Bastian, T. S. 1998, in Astronomical Society of the Pacific Conference Series, Vol. 144
- Bower, G. C., Plambeck, R. L., Bolatto, A., et al. 2003, ApJ, 598, 1140
- Brown, J. M., & Brown, A. 2006, ApJL, 638, L37
- Burton, K., MacGregor, M. A., & Osten, R. A. 2022, ApJL, 939, L6
- Candelaresi, S., Hillier, A., Maehara, H., Brandenburg, A., & Shibata, K. 2014, ApJ, 792, 67,
- Davenport, J. R. A., Covey, K. R., Clarke, R. W., et al. 2019, ApJ, 871, 241
- Dulk, G. A. 1985, ARA&A, 23, 169
- Dzib, S. A., Loinard, L., Rodrıguez, L. F., et al. 2015, ApJ, 801, 91
- Favata, F., Micela, G., & Sciortino, S. 1998, A&A, 337, 413
- Feigelson, E. D., & Montmerle, T. 1999, ARA&A, 37, 363
- Fletcher, L., Dennis, B. R., Hudson, H. S., et al. 2011, SSRv, 159, 19
- Forbrich, J., Reid, M. J., Menten, K. M., et al. 2017, ApJ, 844, 109
- Güdel, M. 2002, ARA&A, 40, 217
- Guns, S., Foster, A., Daley, C., et al. 2021, ApJ, 916, 98
- Howard, W. S., MacGregor, M. A., Osten, R., et al. 2022, ApJ, 938, 103
- Johnstone, D., Lalchand, B., Mairs, S., et al. 2022, ApJ, 937, 6
- Kenyon, S. J., & Bromley, B. C. 2004, AJ, 127, 513
- Lovell, J. B., Wyatt, M. C., Ansdell, M., et al. 2021, MNRAS, 500, 4878
- MacGregor, A. M., Osten, R. A., & Hughes, A. M. 2020, ApJ, 891, 80
- MacGregor, M. A., Weinberger, A. J., Loyd, R. O. P., et al. 2021, ApJL, 911, L25,
- Mairs, S., Lalchand, B., Bower, G. C., et al. 2019, ApJ, 871, 72
- Massi, M., Forbrich, J., Menten, K. M., et al. 2006, A&A, 453, 959
- Massi, M., Ros, E., Menten, K. M., et al. 2008, A&A, 480
- Michel, A., van der Marel, N., & Matthews, B. C. 2021, ApJ, 921, 72
- Morbidelli, A., Lunine, J. I., O'Brien, D. P., Raymond, S. N., & Walsh, K. J. 2012, AREPS, 40, 251
- Naess, S., Battaglia, N., Richard Bond, J., et al. 2021, ApJ, 915, 14
- Salter, D. M., Kóspál, Á., Getman, K. V., et al. 2010, A&A, 521, A32,
- Tilley, M. A., Segura, A., Meadows, V., Hawley, S., &
- Vargas-González, J., Forbrich, J., Dzib, S. A., & Bally, J. 2021, MNRAS, 506, 3169
- Vargas-González, J., Forbrich, J., Rivilla, V. M., et al. 2023, MNRAS, 522, 56

A NOVEL OPTICAL DIPLEXER FOR wSMA DUAL-BAND DUAL POLARIZATION OBSERVATIONS

Edward Tong[1], Keara Carter[1]

The new wSMA cryostat is equipped with an internal 4-position selector wheel. The wheel's primary role is to facilitate user selection between the Low Band (210-270 GHz) and the High Band (280-360 GHz) receiver cartridges. This is made possible through having either an open wheel position or a mirror in the wheel. The configuration of the selector wheel is depicted in Fig. 1 and Table 1 provides the selection matrix corresponding to the wheel's various positions. Beyond these two primary settings, the selector wheel accommodates a wire grid polarizer, which allows the selection of one polarization from each of the two receiver cartridges. The wheel's fourth position is reserved for an optical diplexer, which is instrumental in enabling concurrent operation of both receiver cartridges, opening up the possibility for simultaneous dual-band, dual polarization observations.

A commercially available optical diplexer (also known as dichroic) can be employed to spatially separate the 230 GHz beam from the 345 GHz beam. However, there are two major drawbacks with this off-the-shelf solution. First, it presents a transmission loss of about 8% at 345 GHz. This loss is translated to a noise penalty of approximately 10 K on top of an expected noise temperature of 50 K for the wSMA receiver operating at 345 GHz. Second, the recommended maximum angle of incidence of this diplexer is 22.5 degrees, while the geometry of the wSMA cryostat dictates an incident angle of 30 degrees. As a result, the Receiver Lab has pursued the development of a new low loss optical diplexer tailored for use in the wSMA receiver system.

We have focused our attention on the use of high resistivity silicon disks (HR-Si); a material which is known to have very low loss at 300 GHz and a relatively high refractive in-

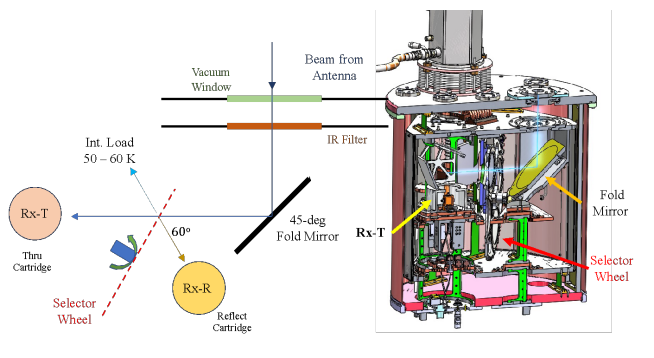

Figure 1: (Left) A schematic representation of the internal layout inside the wSMA cryostat, showing the selector wheel and the pair of Receiver Cartridges (Rx-T and Rx-R). **(Right)** A 3-D model showing the 4-position selector wheel and just the Thru Cartridge (Rx-T).

Selector Element	Rx-T	Rx-R
Unpopulated (Thru)	Active (dual-pol)	X
Mirror	X	Active (dual-pol)
Wire Grid	Active (1-pol)	Active (1-pol)
Diplexer	Active (dual-pol)	Active (dual-pol)

Table 1: Receiver and polarization matrix as a function of which selector element is rotated into the beam inside the cryostat.

[1]Center for Astrophysics | Harvard and Smithsonian

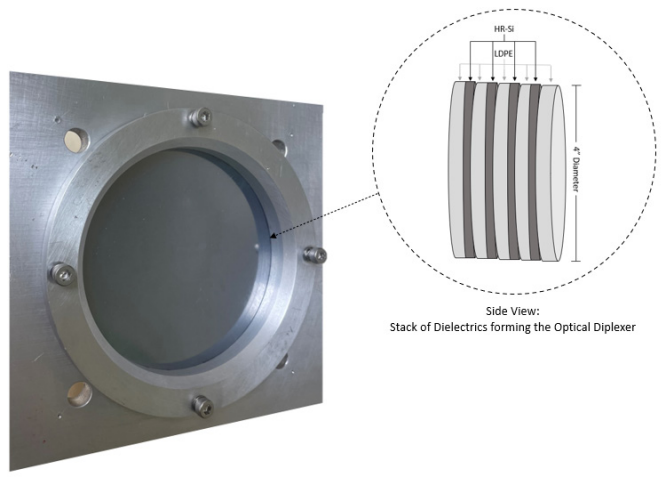

Figure 2: (Left) Optical diplexer installed into a fixture. **(Right)** Side view of the 9-layers of dielectric materials stacked to form the optical diplexer.

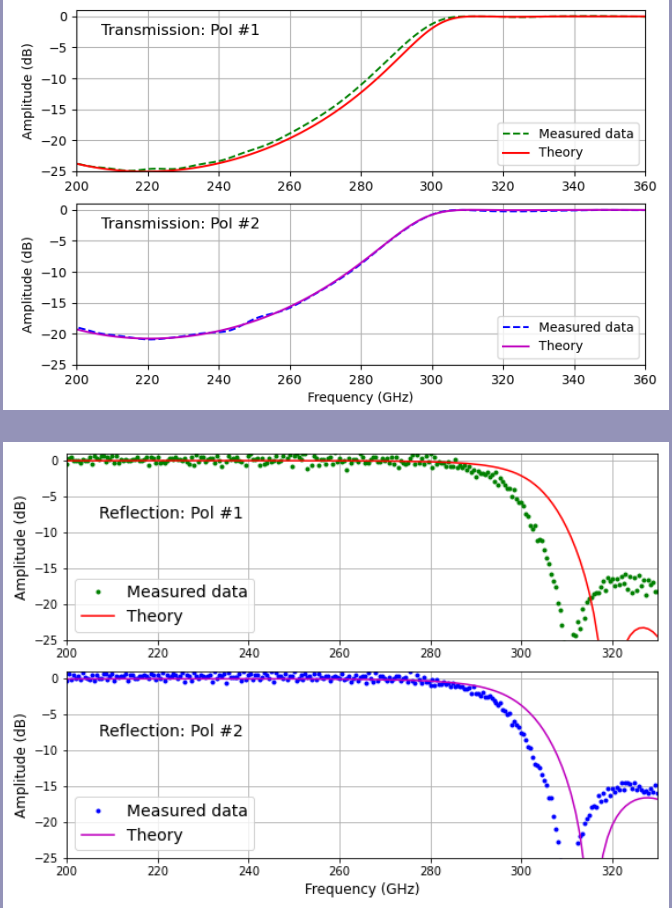

Figure 3: (Top) Transmission characteristics of the optical diplexer as measured by our free space vector analyzer for the 2 different polarizations. **(Bottom)** Measured reflection of the diplexer. The theoretical transmission and reflection data are shown as a comparison. The angle of incidence is 30 degrees.

dex of 3.42. By constructing a dielectric stack composed of alternating layers of HR-Si disks and low-loss Low Density Polyethylene (LDPE) films, we achieved an optical realization of a classical microwave choke filter. This class of filter is characterized by a cascade of low and high impedance sections. In our case, the HR-Si disks act as the low impedance sections and the LDPE films, with a lower refractive index of 1.52, represent the high impedance sections. By varying the thicknesses of the elements of the stack, one can "tune" the reflection and transmission spectra of the diplexer. This process is analytical in nature, as the expressions for the coefficients of reflection and transmission of a dielectric stack are well-documented in textbooks [1]. A diagram of the dielectric stack, and its corresponding application as an optical diplexer, are shown in Fig. 2.

A 9-layer dielectric stack has been constructed and tested. Fig. 3 shows the theoretical and measured transmission and reflection curves when the stack is illuminated by an incident beam at an angle of incidence of 30 degrees. The data set was measured using a free-space vector analyzer with an accuracy of ~0.5 dB. From the plot, we deduce a cross-over frequency of ~295 GHz. Above this frequency, the diplexer is highly transmissive, while below it, the diplexer becomes reflective. There is excellent agreement between the theoretical and measured transmission curves. However, the measured reflections are generally smaller than the expected values above the cross-over frequency. This is linked to the presence of unwanted scattering of the reflected beam in our measurement setup, likely coming from the sidelobes of the horn we used.

These transmission and reflection properties of this dielectric stack meet the optical diplexing requirements of the wSMA system. By introducing the wSMA Low Band receiver as the Reflect cartridge (Rx-R) and the High Band receiver as the Thru cartridge (Rx-T), we can perform dual band observations. The 210-270 GHz band will be covered by Rx-R and frequencies above 320 GHz will be covered by Rx-T.

We have confirmed the low-loss transmission property of this new optical diplexer with the wSMA High Band receiver operating at an LO frequency of 348 GHz. For the measurement, we inserted the dielectric stack in front of the vacuum window, tilted at an angle of 30 degrees with respect to the incident beam. Receiver noise measurements were conducted with and without the stack at various LO drive levels. The data was analyzed using the Method of Intersecting Lines [2]. The results showed an average transmission coefficient of about 97%. This indicates that this optical diplexer is expected to incur only a ~3 K noise penalty on the receiver.

The work with this new class of optical diplexer has so far been conducted at room temperature. Since the coefficients

of contraction of HR-Si and LDPE vary drastically, a tightly bound stack of HR-Si and LDPE may be prone to breakage when cooled to cryogenic temperatures. The next step of development is to test configurations that would allow the dielectric stacks to be mounted in the cryogenic selector wheel of the wSMA cryostat. If successful, the wSMA receiver system will be ready for dual band, dual polarization observations for the SMA.

REFERENCES

- Born, M. and Wolf, E. (1959) Principles of Optics: Electromagnetic Theory of Propagation, Interference, and Diffraction of Light. Cambridge University Press, London.
- C.-Y. Edward Tong, Abby Hedden, and Ray Blundell, "An Empirical Probe to the Operation of SIS Receivers- Revisiting the Technique of Intersecting Lines" in Proc. 19th Int. Symp. Space Tech., pp. 314-318, Gron ingen, Netherlands, Apr. 2008.

EXPANDING HORIZONS: CELEBRATING SMA'S COMMUNITY OUTREACH

We're thrilled to share exciting news with you all! Please join us in extending a warm welcome to Pam Nehls, our newly appointed Education and Engagement Outreach Coordinator. With a wealth of experience in event coordination and community engagement, Pam's expertise will be instrumental as we expand our outreach efforts. In her new role, she'll lead initiatives to connect with the Maunakea Observatories Astronomy Center (MKOAC), schools, community organizations, and the public, with a focus on inspiring the next generation of scientists and deepening our ties within the community.

We're delighted to highlight some of the impactful outreach endeavors we've recently embarked upon. Here's a snapshot of the variety of activities that have allowed us to engage with our community:

Tanabata Japanese Star Festival - August 19, 2023: At the 'Imiloa Astronomy Center, we celebrated the Tanabata Japanese Star Festival, drawing nearly 2,500 attendees. This enchanting event, steeped in folklore, allowed attendees to immerse themselves in the "Story of Tanabata in the Night Sky," fostering a deeper appreciation for astronomy and cultural heritage.

Journey Through the Universe - February 5-9, 2024: Celebrating its 20th year, Journey Through the Universe illuminated classrooms across Hilo, igniting curiosity and passion for science education. Our teams delivered dynamic presentations and career panels, inspiring students from PreK to 7th grade.

Merrie Monarch Parade - April 8, 2024: Representing SMA at the 61st Annual Merrie Monarch Festival Royal Parade, we celebrated Hawaiian culture and shared our passion for astronomy with the community, underscoring our commitment to cultural exchange and community engagement.

Le Jardin Academy Field Trip - April 18, 2024: In collaboration with Gemini Observatory, we hosted 60 fourth-grade students from Le Jardin Academy, providing an immersive educational experience focused on optical and radio telescopes.

AstroDay - May 4, 2024: At AstroDay East Hawaii, we blended science and fun, engaging attendees of all ages with hands-on activities and educational opportunities, celebrating the wonders of astronomy and science education.

(left) Astro Day East: SMA Director Tim Norton and Uncle Kimo Pihana

(right) SMA Booth: John Miller, Adam Mills, Angelu Ramos, and Astro Day Coin Contest winner

We're also excited to announce SMA Hawaii's participation at the upcoming **Astro Bash in Waimea on August 3, 2024**.

We're grateful for the ongoing support of the SMA team and look forward to continuing to foster community bonds and make a positive impact through education and engagement.

If you plan to visit the SMA and would like to share your mana'o, please reach out to Pam Nehls. She'll be delighted to assist you in coordinating any outreach activities during your visit or virtually, too!

Le Jardin Academy Students at the SMA Building in Hilo

BUILDING FOR A BRIGHTER FUTURE: CONSTRUCTION UPDATES AT THE SUBMILLIMETER ARRAY

Exciting developments are underway at the SAO/SMA Submillimeter Array as we continue to enhance our facilities to better serve our mission. Here's a brief overview of our ongoing construction projects:

Backup Generator Building (Hilo Base Facility): In response to Hawaii's unpredictable weather conditions and occasional power outages, we're nearing completion of a new backup generator building at our Hilo Base Facility. Scheduled for completion by August 2024, this addition will ensure uninterrupted power supply, bolstering our resilience against unexpected disruptions. Additionally, it will provide much-needed storage space, improving functionality and convenience for our team.

Active Power System (APS) Project (Maunakea Summit Facility): At our summit facility on Maunakea, we're making significant strides with the Active Power System (APS) project. This project, which features innovative flywheel technology, is currently at a 50% completion rate (new mezzanine installed). Once operational, the APS will safeguard essential systems, ensuring seamless operations even during power outages. Alongside the APS, we're also implementing upgrades such as a new facility water heater and hanger door repair, further enhancing our infrastructure for optimal performance.

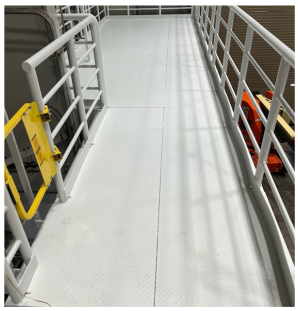

Summit Pavement Project (Maunakea Summit Facility): We're proud to announce the successful completion of the Summit Pavement Project in late 2023. This project has transformed our parking infrastructure, improving accessibility and convenience for our staff, visitors, and heavy equipment.

Summit PACU Project (MaunaKea Summit Facility): Adding to our list of projects, we've recently commenced the Packaged Air Condition Unit (PACU) replacement/upgrade project as of April 2024. The new PACU will provide AC to the correlator room and maintain a designated temperature to ensure the uninterrupted operation of our equipment. The project also encompasses replacing the AC units in our 2nd-floor server room, a comprehensive fire alarm system upgrade, and an updated building management system. With favorable conditions, we aim to complete this project by May 2025.

We extend our sincerest aloha and mahalo to our dedicated team for their hard work and commitment to these projects. Your efforts are instrumental in shaping the future success of the SMA. Stay tuned for more updates as we continue to build a brighter and more resilient future together!

ACKNOWLEDGING THE SMA IN PUBLICATIONS

We would like to remind the community that we request all papers that contain results obtained with data from the Submillimeter Array to include the following observatory acknowledgement (usually in the last section before the references):

> *The Submillimeter Array is a joint project between the Smithsonian Astrophysical Observatory and the Academia Sinica Institute of Astronomy and Astrophysics and is funded by the Smithsonian Institution and the Academia Sinica.*

and we further suggest the following Maunakea site acknowledgement:

> *We recognize that Maunakea is a culturally important site for the indigenous Hawaiian people; we are privileged to study the cosmos from its summit.*

In addition, please use the facility tag **\facility{SMA}** in manuscripts where applicable.

Bibliometrics, while imperfect, are useful in the evaluation and tracking of the observatory's scientific output and impact (e.g. Observatory Bibliographers Collaboration et al. 2023). The SMA observatory acknowledgement and facility tag help to associate publications with the SMA. We maintain a curated library in the SAO/NASA Astrophysics Data System (ADS) of refereed scientific papers as an observatory bibliography. This ADS library, which contains over 1000 papers, may be accessed by a link from the navigation bar on the SMA Observer Center home page. Within ADS this library is searchable in a query by specifying the search term **bibgroup:SMA**.

If you have questions, please contact **sma-pubs@cfa.harvard.edu**

REFERENCES

- Observatory Bibliographers Collaboration, D'Abrusco, R., Gomez, M., et al. 2023, arXiv:2401.00060

CALL FOR STANDARD OBSERVING PROPOSALS – 2024B SEMESTER

The next Call for Standard Observing Proposals for observations with the Submillimeter Array (SMA) is for the 2024B semester with observing period nominally **16 Nov 2024 – 15 May 2025** (subject to adjustment as needed).

The deadline for proposals for the 2024B semester will be:

12 September 2024 3PM Hawaii Standard Time =
12 Sep 2024 9PM Cambridge (EDT)
13 Sep 2024 1AM GMT
13 Sep 2024 3AM CEST
13 Sep 2024 9AM Taipei

Please note the change in the deadline time of day relative to previous calls.

The SMA proposal system will open for users to begin crafting their submissions on or before **August 15** at the SMA Observer Center (SMAOC) at **http://sma1.sma.hawaii.edu/call.html** and will include full details on time available, and the proposal submission process.

Details on the SMA capabilities and status can be found at **http://sma1.sma.hawaii.edu/status.html;** proposal creation and submission is also done through the SMAOC at **http://sma1.sma.hawaii.edu/proposing.html.** We are happy to answer any questions and provide assistance in proposal submission; simply email **sma-propose@cfa.harvard.edu** with any inquiries.

Sincerely,

Mark Gurwell, SAO Chair, SMA TAC; Ya-Wen Tang, ASIAA Chair, SMA TAC

PROPOSAL STATISTICS FOR 2024A

The 2024A proposal deadline was 20:00 UT March 6, 2024. The three SMA partner institutions received a total of 51 proposals (42 SAO, 7 ASIAA, 2 UH.) The 2024A proposals were divided among science categories as follows:

CATEGORY	PROPOSALS
high mass (OB) star formation, cores	10
protoplanetary, transition, debris disks	10
local galaxies, starbursts, AGN	8
low/intermediate mass star formation, cores	7
submm/hi-z galaxies	5
GRB, SN, high energy	4
solar system	3
other	2
evolved stars, AGB, PPN	1
galactic center	1

We note that we are concurrently also running two SAO Large Scale and one ASIAA Key Project programs.

2024A TRACK ALLOCATIONS BY WEATHER REQUIREMENT AND CONFIGURATION:

To best accomodate the highest ranked programs from each of the partners, including Large Scale (SAO) and Key Project (ASIAA) programs it was determined that the configuration schedule will be:

COMPACT >> VERY EXTENDED >> SUBCOMPACT >> EXTENDED >> COMPACT

The very extended configuration will also include some allocated tracks from 2023B, held over to increase efficiency of reconfigurations.

Tracks were allocated in the following manner:

PWV[1]	SAO	ASIAA	UH[2]
< 4.0mm	19A + 39B	0A + 14B	6A
< 2.5mm	14A + 25B	0A + 3B	0
< 1.0mm	2B	0A + 0B	0
Total	**33A + 66B**	**17B**	**6A**

Configuration	SAO	ASIAA	UH
Subcompact	1A + 22B	0A + 2B	6A
Compact	19A + 20B	0A + 6B	0
Extended	2A + 5B	0A + 0B	0
Very Extended	1A + 4B	0A + 0B	0
Any	10A + 15B	0A + 9B	6A
Total	**33A + 66B**	**0A + 17B**	**6A**

(1) Precipitable water vapor required for the observations.

(2) UH allocations are not yet complete.

SAO Large Scale and ASIAA Key Projects are allocated approximately 30 <4.0mm and 35 <2.5mm tracks; one program is a time domain project with variable triggering rates based upon random source activity, thus allocations per semester are somewhat uncertain and could deviate from these expectations.

TOP-RANKED 2024A SEMESTER PROPOSALS

The following is the listing of all SAO and UH proposals with at least one A-rank track allocation. ASIAA allocated only B-rank tracks for their standard proposals for 2024A.

EVOLVED STARS, AGB, PPN

2024A-S010 Joel Kastner, Rochester Institute of Technology
Mapping the Complex Molecular Envelope of the (Iconic) Ring Nebula, NGC 6720

GALACTIC CENTER

2024A-S009 Xing Pan, CfA
What's the role of core-scale magnetic field in the CMZ?

GRB, SN, HIGH ENERGY

2024A-S006 Alexandra Tetarenko, University of Lethbridge
Probing the Jet Response to Neutron Star X-ray Bursts with the SMA

HIGH MASS (OB) STAR FORMATION, CORES

2024A- S001 Qizhou Zhang, CfA
What drives the starburst in W49A?

LOCAL GALAXIES, STARBURSTS, AGN

2024A-S024 Jakob den Brok, CfA
Resolved CO excitation across the Milky-Way Analog Galaxy IC342

2024A-S020 Steven Willner, CfA
Disentangling radiating particle properties and jet physics from M87 multi-wavelength variability (in progress multi-semester program)

OTHER

2024A-S026 Saeqa Vrtilek, CfA
SMA observations of polarization during Microquasar outbursts.

PROTOPLANETARY, TRANSITION, DEBRIS DISKS

2024A-S040 Joshua Lovell, CfA
A giant, eccentric circumbinary disk in Cepheus? Determining the origin of asymmetric substructure in Dracula's disk

2024A-S003 Joshua Lovell, CfA
The Cepheus Hundred: An SMA survey of Cepheus' earliest- type Young Stellar Objects & their planet-forming disks

2024A-H001 Jonathan Williams, UH
A millimeter survey of disks around Herbig stars

SOLAR SYSTEM

2024A-S037 Arielle Moullet, NRAO
Subsurface Thermal Studies of Near-Earth Asteroids

2024A-S033 Nathan Roth, NASA Goddard Space Flight Center
Joint SMA/VLA Studies of Exceptional Comet C/2023 A3

SUBMM/HI-Z GALAXIES

2024A-S028 Garrett "Karto" Keating, SMA/SAO
A Monster, Hiding in the Dark

STANDARD, DDT, AND LARGE SCALE PROJECTS OBSERVED DURING 2023B

SMA Semester 2023B encompassed the period Nov 14, 2023 through May 15, 2024; listed below are projects that were at least partially completed during the semester.

EVOLVED STARS, AGB, PPN

2023B-S004 Joel Kastner, Rochester Institute of Technology
Mapping the Complex Molecular Envelope of the (Iconic) Ring Nebula, NGC 6720

GALACTIC CENTER

2023B-S017 Howard Smith, CfA
SMA Continued Participation in Simultaneous Monitoring, with JWST, of Flaring from the Galactic Center's Supermassive Black Hole

2023B-S052 Garrett "Karto" Keating, CfA
Polarimetric VLBI for the 2024 Event Horizon Telescope Campaign

2023B-S065 Thushara Piillai, MIT Haystack Observatory
*DDT: Multi-frequency Spectral Measurements of G0.02467-0.07, Newly Discovered Compact Source near Sgr A**

GRB, SN, HIGH ENERGY

2022B-S048 Edo Berger, CfA
POETS: Pursuit of Extragalactic Transients with the SMA [SAO Large Scale]

HIGH MASS (OB) STAR FORMATION, CORES

2023A-A012 Seamus Clarke, ASIAA
B-fields, gravity and turbulence across multiple scales - How does the relative importance of gravity, turbulence and magnetic fields impact high-mass star and cluster formation? [ASIAA Key Project]

2023B-A015 Greta Hiu Lam Siu, National Tsing Hua University,
Probing turbulence and magnetic field strength in high mass star forming clumps

LOCAL GALAXIES, STARBURSTS, AGN

2023B-S007 Gerrit Schellenberger, CfA
Are ADAFs the missing link in galaxy cluster and group feedback?

2023B-S008 Gerrit Schellenberger, CfA
Probing the High Frequency Variability of NGC5044: The Key to AGN Feedback

2023B-S016 Kirsten Hall, CfA
Direct, observational evidence of AGN feedback on host galaxies' molecular gas, part 2

2023B-S023 Eric Koch, CfA
Molecular clouds fueling low-density star formation in edge-on systems

2023B-S025 Jakob den Brok, CfA
What drives the unusually high SFR in the elliptical+spiral pair Arp 142?

2023B-S027 Jakob den Brok, CfA
Understanding the cause of the drastic decrease of alphaCO in M101

2023B-S030 Steven Willner, CfA
Disentangling radiating particle properties and jet physics from M87 multi-wavelength variability (in progress multi-semester program)

2023B-S031 Ioannis Myserlis, IRAM
SMAPOL: SMA Monitoring of AGNs with POLarization

2023B-S048 Venkatessh Ramakrishnan, Metsähovi Radio Observatory
Constraining the compactness of accretion flows and jets in low-luminosity AGNs

2023B-S055 Ivana Beslic, LERMA, Observatoire de Paris
Unraveling the Cigar: dense molecular gas across M 82

2023B-S056 Eileen Meyer, University of Maryland, Baltimore County
Probing the nature of the sub-mm continuum in changing-look AGN 1ES 1927+654

2023B-S059 Jakob den Brok, CfA
DDT: Contrasting the dense gas in AGN vs. starburst environment (AY191 student project)

LOW/INTERMEDIATE MASS STAR FORMATION, CORES

2023B-H001 Suchitra Narayanan, IfA, UH
Search for small sulfuretted species in 6 chemically rich class 0 protostars in Perseus

OTHER

2023B-S038 Joshua Lovell, CfA
Millimeter follow-up of radio-detected YSO multiples: Is stellar multiplicity driving class III millimeter variability?

2023B-S043 Kirsten Hall, CfA
Resolved SZ imaging of galaxy cluster cores with the SMA, part 3

2023B-S046 Michael McCollough, CfA
SMA Observations during XRISM and IXPE Observations of Cygnus X-3

PROTOPLANETARY, TRANSITION, DEBRIS DISKS

2022B-S047 Karin Oberg, CfA
SMA-SPEC: the SMA Survey of Protoplanetary disks to Explore their Chemistry [SAO Large Scale]

2023B-A009 Christian Flores, ASIAA
Tidal disruption in the Haro 5-2 quadruple system

2023B-S003 David Wilner, CfA
A 1.3mm Survey of a New Sample of Herbig Be stars (continued)

2023B-S019 Alice Booth, CfA
The planet formation reservoir in photo-evaporating disks

2023B-S021 Joshua Lovell, CfA
The Cepheus Hundred: An SMA survey of Cepheus' earliest- type Young Stellar Objects & their planet-forming disks

2023B-S035 Jenny Calahan, CfA
A Chemical Survey of Outbursting Sources

SOLAR SYSTEM

2023B-S050 Nathan Roth, NASA Goddard Space Flight Center
Coordinated SMA/ALMA Studies of 12P/Pons-Brooks

2023B-S057 Nathan Roth,NASA Goddard Space Flight Center
SMA Wideband Subsurface Thermal Studies of NEAs

SUBMM/HI-Z GALAXIES

2023B-S001 David Clements, Imperial College London
The Brightest Herschel Galaxies: Lensed or Something Else?

2023B-S039 Ian Smail, CEA, Durham
Searching for a dust bar in the z=4.26 galaxy A1489.850.1

2023B-S042 Cristian Vargas, Pontificia Universidad Catolica de Chile
Securing the redshift and gas properties of J0732, an almost complete Einstein ring

2023B-S051 Garrett "Karto" Keating, CfA
A Monster, Hiding in the Dark

RECENT PUBLICATIONS

TITLE: Multiband cross-correlated radio variability of the blazar 3C 279
AUTHOR: Mohana A, K., Gupta, A. C., Marscher, A. P., Sotnikova, Y. V., Jorstad, S. G., Wiita, P. J., Cui, L., Aller, M. F., Aller, H. D., Kovalev, Y. A., Kovalev, Y. Y., Liu, X., Mufakharov, T. V., Popkov, A. V., Mingaliev, M. G., Erkenov, A. K., Nizhelsky, N. A., Tsybulev, P. G., Zhao, W., Weaver, Z. R., Morozova, D. A.
PUBLICATION: *Monthly Notices of the Royal Astronomical Society, 527, 6970-6980*
PUBLICATION DATE: 01/2024
ABSTRACT: *https://ui.adsabs.harvard.edu/abs/2024MNRAS.527.6970M*
DOI: 10.1093/mnras/stad3583

TITLE: IXPE observation of PKS 2155-304 reveals the most highly polarized blazar
AUTHOR: Kouch, P. M., Liodakis, I., Middei, R., Kim, D. E., Tavecchio, F., Marscher, A. P., Marshall, H. L., Ehlert, S. R., Di Gesu, L., Jorstad, S. G., Agudo, I., Madejski, G. M., Romani, R. W., Errando, M., Lindfors, E., Nilsson, K., Toppari, E., Potter, S. B., Imazawa, R., Sasada, M., Fukazawa, Y., Kawabata, K. S., Uemura, M., Mizuno, T., Nakaoka, T., Akitaya, H., McCall, C., Jermak, H. E., Steele, I. A., Myserlis, I., Gurwell, M., Keating, G. K., Rao, R., Kang, S., Lee, S.-S., Kim, S.-H., Cheong, W. Y., Jeong, H.-W., Angelakis, E., Kraus, A., José Aceituno, F., Bonnoli, G., Casanova, V., Escudero, J., Agís-González, B., Husillos, C., Morcuende, D., Otero-Santos, J., Sota, A., Bachev, R., Antonelli, L. A., Bachetti, M., Baldini, L., Baumgartner, W. H., Bellazzini, R., Bianchi, S., Bongiorno, S. D., Bonino, R., Brez, A., Bucciantini, N., Capitanio, F., Castellano, S., Cavazzuti, E., Chen, C.-T., Ciprini, S., Costa, E., De Rosa, A., Del Monte, E., Di Lalla, N., Di Marco, A., Donnarumma, I., Doroshenko, V., Dovčiak, M., Enoto, T., Evangelista, Y., Fabiani, S., Ferrazzoli, R., Garcia, J. A., Gunji, S., Hayashida, K., Heyl, J., Iwakiri, W., Kaaret, P., Karas, V., Kislat, F., Kitaguchi, T., Kolodziejczak, J. J., Krawczynski, H., La Monaca, F., Latronico, L., Maldera, S., Manfreda, A., Marin, F., Marinucci, A., Massaro, F., Matt, G., Mitsuishi, I., Muleri, F., Negro, M., Ng, C.-Y., O'Dell, S. L., Omodei, N., Oppedisano, C., Papitto, A., Pavlov, G. G., Peirson, A. L., Perri, M., Pesce-Rollins, M., Petrucci, P.-O., Pilia, M., Possenti, A., Poutanen, J., Puccetti, S., Ramsey, B. D., Rankin, J., Ratheesh, A., Roberts, O. J., Sgrò, C., Slane, P., Soffitta, P., Spandre, G., Swartz, D. A., Tamagawa, T., Taverna, R., Tawara, Y., Tennant, A. F., Thomas, N. E., Tombesi, F., Trois, A., Tsygankov, S. S., Turolla, R., Vink, J., Weisskopf, M. C., Wu, K., Xie, F., Zane, S.
PUBLICATION: *arXiv e-prints, arXiv:2406.01693*
PUBLICATION DATE: 06/2024
ABSTRACT: *https://ui.adsabs.harvard.edu/abs/2024arXiv240601693K*
DOI: 10.48550/arXiv.2406.01693

TITLE: SMA 200-400 GHz Survey for Dust Properties in the Icy Class II Disks in the Taurus Molecular Cloud
AUTHOR: Chung, C.-Y., Andrews, S. M., Gurwell, M. A., Wright, M., Long, F., Xu, W., Liu, H. B.
PUBLICATION: *arXiv e-prints, arXiv:2405.19867*
PUBLICATION DATE: 05/2024
ABSTRACT: *https://ui.adsabs.harvard.edu/abs/2024arXiv240519867C*
DOI: 10.48550/arXiv.2405.19867

TITLE: The flaring activity of blazar AO 0235+164 during year 2021
AUTHOR: Escudero Pedrosa, J., Agudo, I., Moritz, T., Marscher, A. P., Jorstad, S., Tramacere, A., Casadio, C., Thum, C., Myserlis, I., Sievers, A., Otero-Santos, J., Morcuende, D., López-Coto, R., D'Ammando, F., Bonnoli, G., Gurwell, M., Gómez, J. L., Rao, R., Keating, G.
PUBLICATION: *arXiv e-prints, arXiv:2405.10141*
PUBLICATION DATE: 05/2024
ABSTRACT: *https://ui.adsabs.harvard.edu/abs/2024arXiv240510141E*
DOI: 10.48550/arXiv.2405.10141

TITLE: High-resolution Pan-STARRS and SMA Observations of IRAS 23077+6707: A Giant Edge-on Protoplanetary Disk
AUTHOR: Monsch, K., Lovell, J. B., Berghea, C. T., Edenhofer, G., Keating, G. K., Andrews, S. M., Bayyari, A., Drake, J. J., Wilner, D. J.
PUBLICATION: *The Astrophysical Journal, 967, L2*
PUBLICATION DATE: 05/2024
ABSTRACT: *https://ui.adsabs.harvard.edu/abs/2024ApJ...967L...2M*
DOI: 10.3847/2041-8213/ad3bb0

TITLE: The Molecular Clouds of M31
AUTHOR: Lada, C. J., Forbrich, J., Petitpas, G., Viaene, S.
PUBLICATION: *The Astrophysical Journal, 966, 193*
PUBLICATION DATE: 05/2024
ABSTRACT: *https://ui.adsabs.harvard.edu/abs/2024ApJ...966..193L*
DOI: 10.3847/1538-4357/ad38bf

TITLE: Molecular Gas Tracers in Young and Old Protoplanetary Disks
AUTHOR: Anderson, D. E., Cleeves, L. I., Blake, G. A., Qi, C., Bergin, E. A., Carpenter, J. M., Schwarz, K. R., Thilenius, C., Zhang, K.
PUBLICATION: *The Astrophysical Journal, 966, 84*
PUBLICATION DATE: 05/2024
ABSTRACT: *https://ui.adsabs.harvard.edu/abs/2024ApJ...966...84A*
DOI: 10.3847/1538-4357/ad2fa2

TITLE: Mass Assembly in Massive Star Formation: A Fragmentation Study of ATLASGAL Clumps
AUTHOR: Pandian, J. D., Chatterjee, R., Csengeri, T., Williams, J. P., Wyrowski, F., Menten, K. M.
PUBLICATION: *The Astrophysical Journal, 966, 54*
PUBLICATION DATE: 05/2024
ABSTRACT: *https://ui.adsabs.harvard.edu/abs/2024ApJ...966...54P*
DOI: 10.3847/1538-4357/ad2fc6

TITLE: Insights into the broadband emission of the TeV blazar Mrk 501 during the first X-ray polarization measurements
AUTHOR: MAGIC Collaboration, Abe, S., Abhir, J., Acciari, V. A., Aguasca-Cabot, A., Agudo, I., Aniello, T., Ansoldi, S., Antonelli, L. A., Arbet Engels, A., Arcaro, C., Asano, K., Babić, A., Baquero, A., Barres de Almeida, U., Barrio, J. A., Batković, I., Bautista, A., Baxter, J., Becerra González, J., Bednarek, W., Bernardini, E., Bernardos, M., Bernete, J., Berti, A., Besenrieder, J., Bigongiari, C., Biland, A., Blanch, O., Bonnoli, G., Bošnjak, Ž., Burelli, I., Busetto, G., Campoy-Ordaz, A., Carosi, A., Carosi, R., Carretero-Castrillo, M., Castro-Tirado, A. J., Ceribella, G., Chai, Y., Cifuentes, A., Colombo, E., Contreras, J. L., Cortina, J., Covino, S., D'Amico, G., D'Elia, V., da Vela, P., Dazzi, F., de Angelis, A., de Lotto, B., de Menezes, R., Del Popolo, A., Delfino, M., Delgado, J., Delgado Mendez, C., di Pierro, F., di Venere, L., Dominis Prester, D., Donini, A., Dorner, D., Doro, M., Elsaesser, D., Emery, G., Escudero, J., Fariña, L., Fattorini, A., Foffano, L., Font, L., Fröse, S., Fukazawa, Y., García López, R. J., Garczarczyk, M., Gasparyan, S., Gaug, M., Giesbrecht Paiva, J. G., Giglietto, N., Giordano, F., Gliwny, P., Godinović, N., Gradetzke, T., Grau, R., Green, D., Green, J. G., Günther, P., Hadasch, D., Hahn, A., Hassan, T., Heckmann, L., Herrera, J., Hrupec, D., Hütten, M., Imazawa, R., Ishio, K., Jiménez Martínez, I., Kayanoki, T., Kerszberg, D., Kluge, G. W., Kobayashi, Y., Kouch, P. M., Kubo, H., Kushida, J., Láinez Lezáun, M., Lamastra, A., Leone, F., Lindfors, E., Linhoff, L., Lombardi, S., Longo, F., López-Coto, R., López-Moya, M., López-Oramas, A., Loporchio, S., Lorini, A., Lyard, E., Machado

de Oliveira Fraga, B., Majumdar, P., Makariev, M., Maneva, G., Mang, N., Manganaro, M., Mangano, S., Mannheim, K., Mariotti, M., Martínez, M., Martínez-Chicharro, M., Mas-Aguilar, A., Mazin, D., Menchiari, S., Mender, S., Miceli, D., Miener, T., Miranda, J. M., Mirzoyan, R., Molero González, M., Molina, E., Mondal, H. A., Moralejo, A., Morcuende, D., Nakamori, T., Nanci, C., Neustroev, V., Nigro, C., Nikolić, L., Nilsson, K., Nishijima, K., Njoh Ekoume, T., Noda, K., Nozaki, S., Ohtani, Y., Okumura, A., Otero-Santos, J., Paiano, S., Palatiello, M., Paneque, D., Paoletti, R., Paredes, J. M., Peresano, M., Persic, M., Pihet, M., Pirola, G., Podobnik, F., Prada Moroni, P. G., Prandini, E., Principe, G., Priyadarshi, C., Rhode, W., Ribó, M., Rico, J., Righi, C., Sahakyan, N., Saito, T., Satalecka, K., Saturni, F. G., Schleicher, B., Schmidt, K., Schmuckermaier, F., Schubert, J. L., Schweizer, T., Sciaccaluga, A., Silvestri, G., Sitarek, J., Sobczynska, D., Spolon, A., Stamerra, A., Strišković, J., Strom, D., Suda, Y., Suutarinen, S., Tajima, H., Takahashi, M., Takeishi, R., Tavecchio, F., Temnikov, P., Terauchi, K., Terzić, T., Teshima, M., Tosti, L., Truzzi, S., Tutone, A., Ubach, S., van Scherpenberg, J., Ventura, S., Viale, I., Vigorito, C. F., Vitale, V., Vovk, I., Walter, R., Will, M., Wunderlich, C., Yamamoto, T.

PUBLICATION: *Astronomy and Astrophysics, 685, A117*
PUBLICATION DATE: 05/2024
ABSTRACT: *https://ui.adsabs.harvard.edu/abs/2024A&A...685A.117M*
DOI: 10.1051/0004-6361/202348709

TITLE: Forming localized dust concentrations in a dust ring: DM Tau case study. The asymmetric 7 mm dust continuum of the DM Tau disk
AUTHOR: Liu, H. B., Muto, T., Konishi, M., Chung, C.-Y., Hashimoto, J., Doi, K., Dong, R., Kudo, T., Hasegawa, Y., Terada, Y., Kataoka, A.
PUBLICATION: *Astronomy and Astrophysics, 685, A18*
PUBLICATION DATE: 05/2024
ABSTRACT: *https://ui.adsabs.harvard.edu/abs/2024A&A...685A..18L*
DOI: 10.1051/0004-6361/202348896

TITLE: Broadband Multi-wavelength Properties of M87 during the 2018 EHT Campaign including a Very High Energy Flaring Episode
AUTHOR: The Event Horizon Telescope-Multi-wavelength science working group, The Event Horizon Telescope Collaboration, The Fermi Large Area Telescope Collaboration, H. E. S. S. Collaboration, MAGIC Collaboration, VERITAS Collaboration, EAVN Collaboration
PUBLICATION: *arXiv e-prints, arXiv:2404.17623*
PUBLICATION DATE: 04/2024
ABSTRACT: *https://ui.adsabs.harvard.edu/abs/2024arXiv240417623T*
DOI: 10.48550/arXiv.2404.17623

TITLE: Measurements of Titan's Stratospheric Winds during the 2009 Equinox with the eSMA
AUTHOR: Light, S., Gurwell, M., Thelen, A., Lombardo, N. A., Nixon, C.
PUBLICATION: *The Planetary Science Journal, 5, 98*
PUBLICATION DATE: 04/2024
ABSTRACT: *https://ui.adsabs.harvard.edu/abs/2024PSJ.....5...98L*
DOI: 10.3847/PSJ/ad3355

TITLE: The Molecular Exoskeleton of the Ring-like Planetary Nebula NGC 3132
AUTHOR: Kastner, J. H., Wilner, D. J., Moraga Baez, P., Bublitz, J., De Marco, O., Sahai, R., Wootten, A.
PUBLICATION: *The Astrophysical Journal, 965, 21*
PUBLICATION DATE: 04/2024
ABSTRACT: *https://ui.adsabs.harvard.edu/abs/2024ApJ...965...21K*
DOI: 10.3847/1538-4357/ad2848

TITLE: First Sagittarius A* Event Horizon Telescope Results. VIII. Physical Interpretation of the Polarized Ring

AUTHOR: Event Horizon Telescope Collaboration, Akiyama, K., Alberdi, A., Alef, W., Algaba, J. C., Anantua, R., Asada, K., Azulay, R., Bach, U., Baczko, A.-K., Ball, D., Baloković, M., Bandyopadhyay, B., Barrett, J., Bauböck, M., Benson, B. A., Bintley, D., Blackburn, L., Blundell, R., Bouman, K. L., Bower, G. C., Boyce, H., Bremer, M., Brinkerink, C. D., Brissenden, R., Britzen, S., Broderick, A. E., Broguiere, D., Bronzwaer, T., Bustamante, S., Byun, D.-Y., Carlstrom, J. E., Ceccobello, C., Chael, A., Chan, C.-. kwan ., Chang, D. O., Chatterjee, K., Chatterjee, S., Chen, M.-T., Chen, Y., Cheng, X., Cho, I., Christian, P., Conroy, N. S., Conway, J. E., Cordes, J. M., Crawford, T. M., Crew, G. B., Cruz-Osorio, A., Cui, Y., Dahale, R., Davelaar, J., De Laurentis, M., Deane, R., Dempsey, J., Desvignes, G., Dexter, J., Dhruv, V., Dihingia, I. K., Doeleman, S. S., Dougall, S., Dzib, S. A., Eatough, R. P., Emami, R., Falcke, H., Farah, J., Fish, V. L., Fomalont, E., Ford, H. A., Foschi, M., Fraga-Encinas, R., Freeman, W. T., Friberg, P., Fromm, C. M., Fuentes, A., Galison, P., Gammie, C. F., García, R., Gentaz, O., Georgiev, B., Goddi, C., Gold, R., Gómez-Ruiz, A. I., Gómez, J. L., Gu, M., Gurwell, M., Hada, K., Haggard, D., Haworth, K., Hecht, M. H., Hesper, R., Heumann, D., Ho, L. C., Ho, P., Honma, M., Huang, C.-W. L., Huang, L., Hughes, D. H., Ikeda, S., Impellizzeri, C. M. V., Inoue, M., Issaoun, S., James, D. J., Jannuzi, B. T., Janssen, M., Jeter, B., Jiang, W., Jiménez-Rosales, A., Johnson, M. D., Jorstad, S., Joshi, A. V., Jung, T., Karami, M., Karuppusamy, R., Kawashima, T., Keating, G. K., Kettenis, M., Kim, D.-J., Kim, J.-Y., Kim, J., Kim, J., Kino, M., Koay, J. Y., Kocherlakota, P., Kofuji, Y., Koch, P. M., Koyama, S., Kramer, C., Kramer, J. A., Kramer, M., Krichbaum, T. P., Kuo, C.-Y., La Bella, N., Lauer, T. R., Lee, D., Lee, S.-S., Leung, P. K., Levis, A., Li, Z., Lico, R., Lindahl, G., Lindqvist, M., Lisakov, M., Liu, J., Liu, K., Liuzzo, E., Lo, W.-P., Lobanov, A. P., Loinard, L., Lonsdale, C. J., Lowitz, A. E., Lu, R.-S., MacDonald, N. R., Mao, J., Marchili, N., Markoff, S., Marrone, D. P., Marscher, A. P., Martí-Vidal, I., Matsushita, S., Matthews, L. D., Medeiros, L., Menten, K. M., Michalik, D., Mizuno, I., Mizuno, Y., Moran, J. M., Moriyama, K., Moscibrodzka, M., Mulaudzi, W., Müller, C., Müller, H., Mus, A., Musoke, G., Myserlis, I., Nadolski, A., Nagai, H., Nagar, N. M., Nakamura, M., Narayanan, G., Natarajan, I., Nathanail, A., Fuentes, S. N., Neilsen, J., Neri, R., Ni, C., Noutsos, A., Nowak, M. A., Oh, J., Okino, H., Olivares, H., Ortiz-León, G. N., Oyama, T., Özel, F., Palumbo, D. C. M., Paraschos, G. F., Park, J., Parsons, H., Patel, N., Pen, U.-L., Pesce, D. W., Piétu, V., Plambeck, R., PopStefanija, A., Porth, O., Pötzl, F. M., Prather, B., Preciado-López, J. A., Psaltis, D., Pu, H.-Y., Ramakrishnan, V., Rao, R., Rawlings, M. G., Raymond, A. W., Rezzolla, L., Ricarte, A., Ripperda, B., Roelofs, F., Rogers, A., Romero-Cañizales, C., Ros, E., Roshanineshat, A., Rottmann, H., Roy, A. L., Ruiz, I., Ruszczyk, C., Rygl, K. L. J., Sánchez, S., Sánchez-Argüelles, D., Sánchez-Portal, M., Sasada, M., Satapathy, K., Savolainen, T., Schloerb, F. P., Schonfeld, J., Schuster, K.-F., Shao, L., Shen, Z., Small, D., Sohn, B. W., SooHoo, J., Sosapanta Salas, L. D., Souccar, K., Stanway, J. S., Sun, H., Tazaki, F., Tetarenko, A. J., Tiede, P., Tilanus, R. P. J., Titus, M., Torne, P., Toscano, T., Traianou, E., Trent, T., Trippe, S., Turk, M., van Bemmel, I., van Langevelde, H. J., van Rossum, D. R., Vos, J., Wagner, J., Ward-Thompson, D., Wardle, J., Washington, J. E., Weintroub, J., Wharton, R., Wielgus, M., Wiik, K., Witzel, G., Wondrak, M. F., Wong, G. N., Wu, Q., Yadlapalli, N., Yamaguchi, P., Yfantis, A., Yoon, D., Young, A., Young, K., Younsi, Z., Yu, W., Yuan, F., Yuan, Y.-F., Zensus, J. A., Zhang, S., Zhao, G.-Y., Zhao, S.-S., Najafi-Ziyazi, M.

PUBLICATION: *The Astrophysical Journal, 964, L26*

PUBLICATION DATE: 04/2024

ABSTRACT: *https://ui.adsabs.harvard.edu/abs/2024ApJ...964L..26E*

DOI: 10.3847/2041-8213/ad2df1

TITLE: First Sagittarius A* Event Horizon Telescope Results. VII. Polarization of the Ring

AUTHOR: Event Horizon Telescope Collaboration, Akiyama, K., Alberdi, A., Alef, W., Algaba, J. C., Anantua, R., Asada, K., Azulay, R., Bach, U., Baczko, A.-K., Ball, D., Balokovic, M., Bandyopadhyay, B., Barrett, J., Bauböck, M., Benson, B. A., Bintley, D., Blackburn, L., Blundell, R., Bouman, K. L., Bower, G. C., Boyce, H., Bremer, M., Brinkerink, C. D., Brissenden, R., Britzen, S., Broderick, A. E., Broguiere, D., Bronzwaer, T., Bustamante, S., Byun, D.-Y., Carlstrom, J. E., Ceccobello, C., Chael, A., Chan, C.-. kwan ., Chang, D. O., Chatterjee, K., Chatterjee, S., Chen, M.-T., Chen, Y., Cheng, X., Cho, I., Christian, P., Conroy, N. S., Conway, J. E., Cordes, J. M., Crawford, T. M., Crew, G. B., Cruz-Osorio, A., Cui, Y., Dahale, R., Davelaar, J., De Laurentis, M., Deane, R., Dempsey, J., Desvignes, G., Dexter, J., Dhruv, V., Dihingia, I. K., Doeleman, S. S., Dougal, S. T., Dzib, S. A., Eatough, R. P., Emami, R., Falcke, H., Farah, J., Fish, V. L., Fomalont, E., Ford, H. A., Foschi, M., Fraga-Encinas, R., Freeman, W. T., Friberg, P., Fromm, C. M., Fuentes, A., Galison, P., Gammie, C. F., García, R., Gentaz, O., Georgiev, B., Goddi, C., Gold, R., Gómez-Ruiz, A. I., Gómez, J. L., Gu, M., Gurwell, M., Hada, K., Haggard, D., Haworth, K., Hecht, M. H., Hesper, R., Heumann, D., Ho, L. C., Ho, P., Honma, M., Huang, C.-W. L., Huang, L., Hughes, D. H., Ikeda, S., Impellizzeri, C. M. V., Inoue, M., Issaoun, S., James, D. J., Jannuzi, B. T., Janssen, M., Jeter, B., Jiang, W., Jiménez-Rosales, A., Johnson, M. D., Jorstad, S., Joshi, A. V., Jung, T., Karami, M., Karuppusamy, R., Kawashima, T., Keating,

G. K., Kettenis, M., Kim, D.-J., Kim, J.-Y., Kim, J., Kim, J., Kino, M., Koay, J. Y., Kocherlakota, P., Kofuji, Y., Koch, P. M., Koyama, S., Kramer, C., Kramer, J. A., Kramer, M., Krichbaum, T. P., Kuo, C.-Y., La Bella, N., Lauer, T. R., Lee, D., Lee, S.-S., Leung, P. K., Levis, A., Li, Z., Lico, R., Lindahl, G., Lindqvist, M., Lisakov, M., Liu, J., Liu, K., Liuzzo, E., Lo, W.-P., Lobanov, A. P., Loinard, L., Lonsdale, C. J., Lowitz, A. E., Lu, R.-S., MacDonald, N. R., Mao, J., Marchili, N., Markoff, S., Marrone, D. P., Marscher, A. P., Martí-Vidal, I., Matsushita, S., Matthews, L. D., Medeiros, L., Menten, K. M., Michalik, D., Mizuno, I., Mizuno, Y., Moran, J. M., Moriyama, K., Moscibrodzka, M., Mulaudzi, W., Müller, C., Müller, H., Mus, A., Musoke, G., Myserlis, I., Nadolski, A., Nagai, H., Nagar, N. M., Nakamura, M., Narayanan, G., Natarajan, I., Nathanail, A., Fuentes, S. N., Neilsen, J., Neri, R., Ni, C., Noutsos, A., Nowak, M. A., Oh, J., Okino, H., Olivares, H., Ortiz-León, G. N., Oyama, T., Özel, F., Palumbo, D. C. M., Paraschos, G. F., Park, J., Parsons, H., Patel, N., Pen, U.-L., Pesce, D. W., Piétu, V., Plambeck, R., PopStefanija, A., Porth, O., Pötzl, F. M., Prather, B., Preciado-López, J. A., Psaltis, D., Pu, H.-Y., Ramakrishnan, V., Rao, R., Rawlings, M. G., Raymond, A. W., Rezzolla, L., Ricarte, A., Ripperda, B., Roelofs, F., Rogers, A., Romero-Cañizales, C., Ros, E., Roshanineshat, A., Rottmann, H., Roy, A. L., Ruiz, I., Ruszczyk, C., Rygl, K. L. J., Sánchez, S., Sánchez-Argüelles, D., Sánchez-Portal, M., Sasada, M., Satapathy, K., Savolainen, T., Schloerb, F. P., Schonfeld, J., Schuster, K.-F., Shao, L., Shen, Z., Small, D., Sohn, B. W., SooHoo, J., Sosapanta Salas, L. D., Souccar, K., Stanway, J. S., Sun, H., Tazaki, F., Tetarenko, A. J., Tiede, P., Tilanus, R. P. J., Titus, M., Torne, P., Toscano, T., Traianou, E., Trent, T., Trippe, S., Turk, M., van Bemmel, I., van Langevelde, H. J., van Rossum, D. R., Vos, J., Wagner, J., Ward-Thompson, D., Wardle, J., Washington, J. E., Weintroub, J., Wharton, R., Wielgus, M., Wiik, K., Witzel, G., Wondrak, M. F., Wong, G. N., Wu, Q., Yadlapalli, N., Yamaguchi, P., Yfantis, A., Yoon, D., Young, A., Young, K., Younsi, Z., Yu, W., Yuan, F., Yuan, Y.-F., Zensus, J. A., Zhang, S., Zhao, G.-Y., Zhao, S.-S.

PUBLICATION: *The Astrophysical Journal, 964, L25*
PUBLICATION DATE: 04/2024
ABSTRACT: *https://ui.adsabs.harvard.edu/abs/2024ApJ...964L..25E*
DOI: 10.3847/2041-8213/ad2df0

TITLE: Surveys of clumps, cores, and condensations in Cygnus-X. Searching for circumstellar disks
AUTHOR: Pan, X., Qiu, K., Yang, K., Cao, Y., Zhang, X.
PUBLICATION: *Astronomy and Astrophysics, 684, A141*
PUBLICATION DATE: 04/2024
ABSTRACT: *https://ui.adsabs.harvard.edu/abs/2024A&A...684A.141P*
DOI: 10.1051/0004-6361/202346763

TITLE: Microwave spectra of the leading and trailing hemispheres of Iapetus
AUTHOR: Bonnefoy, L. E., Lellouch, E., Le Gall, A., Lestrade, J.-F., Moreno, R., Butler, B., Boissier, J., Leyrat, C., Sultana, R., Cavalié, T., Gurwell, M., Moullet, A., Ladjelate, B., Ponthieu, N.
PUBLICATION: *Icarus, 411, 115950*
PUBLICATION DATE: 03/2024
ABSTRACT: *https://ui.adsabs.harvard.edu/abs/2024Icar..41115950B*
DOI: 10.1016/j.icarus.2024.115950

TITLE: The Jet and Resolved Features of the Central Supermassive Black Hole of M87 Observed with EHT in 2017—Comparison with the GMVA 86 GHz Results
AUTHOR: Miyoshi, M., Kato, Y., Makino, J., Tsuboi, M.
PUBLICATION: *The Astrophysical Journal, 963, L18*
PUBLICATION DATE: 03/2024
ABSTRACT: *https://ui.adsabs.harvard.edu/abs/2024ApJ...963L..18M*
DOI: 10.3847/2041-8213/ad250e

TITLE: Detection of X-Ray Polarization from the Blazar 1ES 1959+650 with the Imaging X-Ray Polarimetry Explorer

AUTHOR: Errando, M., Liodakis, I., Marscher, A. P., Marshall, H. L., Middei, R., Negro, M., Peirson, A. L., Perri, M., Puccetti, S., Rabinowitz, P. L., Agudo, I., Jorstad, S. G., Savchenko, S. S., Blinov, D., Bourbah, I. G., Kiehlmann, S., Kontopodis, E., Mandarakas, N., Romanopoulos, S., Skalidis, R., Vervelaki, A., Aceituno, F. J., Bernardos, M. I., Bonnoli, G., Casanova, V., Agís-González, B., Husillos, C., Marchini, A., Sota, A., Kouch, P. M., Lindfors, E., Casadio, C., Escudero, J., Myserlis, I., Imazawa, R., Sasada, M., Fukazawa, Y., Kawabata, K. S., Uemura, M., Mizuno, T., Nakaoka, T., Akitaya, H., Gurwell, M., Keating, G. K., Rao, R., Ingram, A., Massaro, F., Antonelli, L. A., Bonino, R., Cavazzuti, E., Chen, C.-T., Cibrario, N., Ciprini, S., De Rosa, A., Di Gesu, L., Di Pierro, F., Donnarumma, I., Ehlert, S. R., Fenu, F., Gau, E., Karas, V., Kim, D. E., Krawczynski, H., Laurenti, M., Lisalda, L., López-Coto, R., Madejski, G., Marin, F., Marinucci, A., Mitsuishi, I., Muleri, F., Pacciani, L., Paggi, A., Petrucci, P.-O., Rodriguez Cavero, N., Romani, R. W., Tavecchio, F., Tugliani, S., Wu, K., Bachetti, M., Baldini, L., Baumgartner, W. H., Bellazzini, R., Bianchi, S., Bongiorno, S. D., Brez, A., Bucciantini, N., Capitanio, F., Castellano, S., Costa, E., Del Monte, E., Di Lalla, N., Di Marco, A., Doroshenko, V., Dovčiak, M., Enoto, T., Evangelista, Y., Fabiani, S., Ferrazzoli, R., Garcia, J. A., Gunji, S., Hayashida, K., Heyl, J., Iwakiri, W., Kaaret, P., Kislat, F., Kitaguchi, T., Kolodziejczak, J. J., La Monaca, F., Latronico, L., Maldera, S., Manfreda, A., Matt, G., Ng, C.-Y., O'Dell, S. L., Omodei, N., Oppedisano, C., Papitto, A., Pavlov, G. G., Pesce-Rollins, M., Pilia, M., Possenti, A., Poutanen, J., Ramsey, B. D., Rankin, J., Ratheesh, A., Roberts, O. J., Sgrò, C., Slane, P., Soffitta, P., Spandre, G., Swartz, D. A., Tamagawa, T., Taverna, R., Tawara, Y., Tennant, A. F., Thomas, N. E., Tombesi, F., Trois, A., Tsygankov, S. S., Turolla, R., Vink, J., Weisskopf, M. C., Xie, F., Zane, S.

PUBLICATION: *The Astrophysical Journal, 963, 5*

PUBLICATION DATE: 03/2024

ABSTRACT: *https://ui.adsabs.harvard.edu/abs/2024ApJ...963....5E*

DOI: 10.3847/1538-4357/ad1ce4

TITLE: SMA Detection of an Extreme Millimeter Flare from the Young Class III Star HD 283572

AUTHOR: Lovell, J. B., Keating, G. K., Wilner, D. J., Andrews, S. M., MacGregor, M., Rahman, R. A., Rao, R., Williams, J. P.

PUBLICATION: *The Astrophysical Journal, 962, L12*

PUBLICATION DATE: 02/2024

ABSTRACT: *https://ui.adsabs.harvard.edu/abs/2024ApJ...962L..12L*

DOI: 10.3847/2041-8213/ad18ba

TITLE: Ordered magnetic fields around the 3C 84 central black hole

AUTHOR: Paraschos, G. F., Kim, J.-Y., Wielgus, M., Röder, J., Krichbaum, T. P., Ros, E., Agudo, I., Myserlis, I., Moscibrodzka, M., Traianou, E., Zensus, J. A., Blackburn, L., Chan, C.-K., Issaoun, S., Janssen, M., Johnson, M. D., Fish, V. L., Akiyama, K., Alberdi, A., Alef, W., Algaba, J. C., Anantua, R., Asada, K., Azulay, R., Bach, U., Baczko, A.-K., Ball, D., Baloković, M., Barrett, J., Bauböck, M., Benson, B. A., Bintley, D., Blundell, R., Bouman, K. L., Bower, G. C., Boyce, H., Bremer, M., Brinkerink, C. D., Brissenden, R., Britzen, S., Broderick, A. E., Broguiere, D., Bronzwaer, T., Bustamante, S., Byun, D.-Y., Carlstrom, J. E., Ceccobello, C., Chael, A., Chang, D. O., Chatterjee, K., Chatterjee, S., Chen, M. T., Chen, Y., Cheng, X., Cho, I., Christian, P., Conroy, N. S., Conway, J. E., Cordes, J. M., Crawford, T. M., Crew, G. B., Cruz-Osorio, A., Cui, Y., Dahale, R., Davelaar, J., De Laurentis, M., Deane, R., Dempsey, J., Desvignes, G., Dexter, J., Dhruv, V., Doeleman, S. S., Dougal, S., Dzib, S. A., Eatough, R. P., Emami, R., Falcke, H., Farah, J., Fomalont, E., Ford, H. A., Foschi, M., Fraga-Encinas, R., Freeman, W. T., Friberg, P., Fromm, C. M., Fuentes, A., Galison, P., Gammie, C. F., García, R., Gentaz, O., Georgiev, B., Goddi, C., Gold, R., Gómez-Ruiz, A. I., Gómez, J. L., Gu, M., Gurwell, M., Hada, K., Haggard, D., Haworth, K., Hecht, M. H., Hesper, R., Heumann, D., Ho, L. C., Ho, P., Honma, M., Huang, C. L., Huang, L., Hughes, D. H., Ikeda, S., Impellizzeri, C. M. V., Inoue, M., James, D. J., Jannuzi, B. T., Jeter, B., Jaing, W., Jiménez-Rosales, A., Jorstad, S., Joshi, A. V., Jung, T., Karami, M., Karuppusamy, R., Kawashima, T., Keating, G. K., Kettenis, M., Kim, D.-J., Kim, J., Kim, J., Kino, M., Koay, J. Y., Kocherlakota, P., Kofuji, Y., Koch, P. M., Koyama, S., Kramer, C., Kramer, J. A., Kramer, M., Kuo, C.-Y., La Bella, N., Lauer, T. R., Lee, D., Lee, S.-S., Leung, P. K., Levis, A., Li, Z., Lico, R., Lindahl, G., Lindqvist, M., Lisakov, M., Liu, J., Liu, K., Liuzzo, E., Lo, W.-P., Lobanov, A. P., Loinard, L., Lonsdale, C. J., Lowitz, A. E., Lu, R.-S., MacDonald, N. R., Mao, J., Marchili, N., Markoff, S., Marrone, D. P., Marscher, A. P., Martí-Vidal, I., Matsushita, S., Matthews, L. D., Medeiros, L., Menten, K. M., Michalik, D., Mizuno, I., Mizuno, Y., Moran, J. M., Moriyama, K., Mulaudzi, W., Müller, C., Müller, H., Mus, A., Musoke, G., Nadolski, A., Nagai, H., Nagar, N. M., Nakamura, M., Narayanan, G., Natarajan, I., Nathanail, A., Navarro Fuentes, S., Neilsen, J., Neri, R., Ni, C., Noutsos, A., Nowak, M. A., Oh, J., Okino, H., Olivares, H., Ortiz-León, G. N.,

Oyama, T., Özel, F., Palumbo, D. C. M., Park, J., Parsons, H., Patel, N., Pen, U.-L., Piétu, V., Plambeck, R., PopStefanija, A., Porth, O., Pötzl, F. M., Prather, B., Preciado-López, J. A., Psaltis, D., Pu, H.-Y., Ramakrishnan, V., Rao, R., Rawlings, M. G., Raymond, A. W., Rezzolla, L., Ricarte, A., Ripperda, B., Roelofs, F., Rogers, A., Romero-Cañizales, C., Roshanineshat, A., Rottmann, H., Roy, A. L., Ruiz, I., Ruszczyk, C., Rygl, K. L. J., Sánchez, S., Sánchez-Argüelles, D., Sánchez-Portal, M., Sasada, M., Satapathy, K., Savolainen, T., Schloerb, F. P., Schonfeld, J., Schuster, K., Shao, L., Shen, Z., Small, D., Sohn, B. W., SooHoo, J., Sosapanta Salas, L. D., Souccar, K., Sun, H., Tazaki, F., Tetarenko, A. J., Tiede, P., Tilanus, R. P. J., Titus, M., Torne, P., Toscano, T., Trent, T., Trippe, S., Turk, M., van Bemmel, I., van Langevelde, H. J., van Rossum, D. R., Vos, J., Wagner, J., Ward-Thompson, D., Wardle, J., Washington, J. E., Weintroub, J., Wharton, R., Wiik, K., Witzel, G., Wondrak, M. F., Wong, G. N., Wu, Q., Yadlapalli, N., Yamaguchi, P., Yfantis, A., Yoon, D., Young, A., Young, K., Younsi, Z., Yu, W., Yuan, F., Yuan, Y.-F., Zhang, S., Zhao, G. Y., Zhao, S.-S.

PUBLICATION: *Astronomy and Astrophysics, 682, L3*
PUBLICATION DATE: 02/2024
ABSTRACT: *https://ui.adsabs.harvard.edu/abs/2024A&A...682L...3P*
DOI: 10.1051/0004-6361/202348308

TITLE: The persistent shadow of the supermassive black hole of M 87. I. Observations, calibration, imaging, and analysis
AUTHOR: Event Horizon Telescope Collaboration, Akiyama, K., Alberdi, A., Alef, W., Algaba, J. C., Anantua, R., Asada, K., Azulay, R., Bach, U., Baczko, A.-K., Ball, D., Baloković, M., Bandyopadhyay, B., Barrett, J., Bauböck, M., Benson, B. A., Bintley, D., Blackburn, L., Blundell, R., Bouman, K. L., Bower, G. C., Boyce, H., Bremer, M., Brissenden, R., Britzen, S., Broderick, A. E., Broguiere, D., Bronzwaer, T., Bustamante, S., Carlstrom, J. E., Chael, A., Chan, C.-. kwan ., Chang, D. O., Chatterjee, K., Chatterjee, S., Chen, M.-T., Chen, Y., Cheng, X., Cho, I., Christian, P., Conroy, N. S., Conway, J. E., Crawford, T. M., Crew, G. B., Cruz-Osorio, A., Cui, Y., Dahale, R., Davelaar, J., De Laurentis, M., Deane, R., Dempsey, J., Desvignes, G., Dexter, J., Dhruv, V., Dihingia, I. K., Doeleman, S. S., Dzib, S. A., Eatough, R. P., Emami, R., Falcke, H., Farah, J., Fish, V. L., Fomalont, E., Ford, H. A., Foschi, M., Fraga-Encinas, R., Freeman, W. T., Friberg, P., Fromm, C. M., Fuentes, A., Galison, P., Gammie, C. F., García, R., Gentaz, O., Georgiev, B., Goddi, C., Gold, R., Gómez-Ruiz, A. I., Gómez, J. L., Gu, M., Gurwell, M., Hada, K., Haggard, D., Hesper, R., Heumann, D., Ho, L. C., Ho, P., Honma, M., Huang, C.-W. L., Huang, L., Hughes, D. H., Ikeda, S., Violette Impellizzeri, C. M., Inoue, M., Issaoun, S., James, D. J., Jannuzi, B. T., Janssen, M., Jeter, B., Jiang, W., Jiménez-Rosales, A., Johnson, M. D., Jorstad, S., Jones, A. C., Joshi, A. V., Jung, T., Karuppusamy, R., Kawashima, T., Keating, G. K., Kettenis, M., Kim, D.-J., Kim, J.-Y., Kim, J., Kim, J., Kino, M., Koay, J. Y., Kocherlakota, P., Kofuji, Y., Koch, P. M., Koyama, S., Kramer, C., Kramer, J. A., Kramer, M., Krichbaum, T. P., Kuo, C.-Y., La Bella, N., Lee, S.-S., Levis, A., Li, Z., Lico, R., Lindahl, G., Lindqvist, M., Lisakov, M., Liu, J., Liu, K., Liuzzo, E., Lo, W.-P., Lobanov, A. P., Loinard, L., Lonsdale, C. J., Lowitz, A. E., Lu, R.-S., MacDonald, N. R., Mao, J., Marchili, N., Markoff, S., Marrone, D. P., Marscher, A. P., Martí-Vidal, I., Matsushita, S., Matthews, L. D., Medeiros, L., Menten, K. M., Mizuno, I., Mizuno, Y., Montgomery, J., Moran, J. M., Moriyama, K., Moscibrodzka, M., Mulaudzi, W., Müller, C., Müller, H., Mus, A., Musoke, G., Myserlis, I., Nagai, H., Nagar, N. M., Nakamura, M., Narayanan, G., Natarajan, I., Nathanail, A., Fuentes, S. N., Neilsen, J., Ni, C., Nowak, M. A., Oh, J., Okino, H., Olivares, H., Oyama, T., Özel, F., Palumbo, D. C. M., Paraschos, G. F., Park, J., Parsons, H., Patel, N., Pen, U.-L., Pesce, D. W., Piétu, V., PopStefanija, A., Porth, O., Prather, B., Psaltis, D., Pu, H.-Y., Ramakrishnan, V., Rao, R., Rawlings, M. G., Raymond, A. W., Rezzolla, L., Ricarte, A., Ripperda, B., Roelofs, F., Romero-Cañizales, C., Ros, E., Roshanineshat, A., Rottmann, H., Roy, A. L., Ruiz, I., Ruszczyk, C., Rygl, K. L. J., Sánchez, S., Sánchez-Argüelles, D., Sánchez-Portal, M., Sasada, M., Satapathy, K., Savolainen, T., Schloerb, F. P., Schonfeld, J., Schuster, K.-F., Shao, L., Shen, Z., Small, D., Sohn, B. W., SooHoo, J., Salas, L. D. S., Souccar, K., Stanway, J. S., Sun, H., Tazaki, F., Tetarenko, A. J., Tiede, P., Tilanus, R. P. J., Titus, M., Toma, K., Torne, P., Toscano, T., Traianou, E., Trent, T., Trippe, S., Turk, M., van Bemmel, I., van Langevelde, H. J., van Rossum, D. R., Vos, J., Wagner, J., Ward-Thompson, D., Wardle, J., Washington, J. E., Weintroub, J., Wharton, R., Wielgus, M., Wiik, K., Witzel, G., Wondrak, M. F., Wong, G. N., Wu, Q., Yadlapalli, N., Yamaguchi, P., Yfantis, A., Yoon, D., Young, A., Younsi, Z., Yu, W., Yuan, F., Yuan, Y.-F., Anton Zensus, J., Zhang, S., Zhao, G.-Y., Zhao, S.-S., Allardi, A., Chang, S.-H., Chang, C.-C., Chang, S.-C., Chen, C.-C., Chilson, R., Faber, A., Gale, D. M., Han, C.-C., Han, K.-C., Hasegawa, Y., Hernández-Rebollar, J. L., Huang, Y.-D., Jiang, H., Jinchi, H., Kimura, K., Kubo, D., Li, C.-T., Lin, L. C.-C., Liu, C.-T., Liu, K.-Y., Lu, L.-M., Martin-Cocher, P., Meyer-Zhao, Z., Montaña, A., Moraghan, A., Moreno-Nolasco, M. E., Nishioka, H., Norton, T. J., Nystrom, G., Ogawa, H., Oshiro, P., Pradel, N., Principe, G., Raffin, P., Rodríguez-Montoya, I., Shaw, P., Snow, W., Sridharan, T. K., Srinivasan, R., Wei, T.-S., Yu, C.-Y.

PUBLICATION: *Astronomy and Astrophysics, 681, A79*
PUBLICATION DATE: 01/2024
ABSTRACT: *https://ui.adsabs.harvard.edu/abs/2024A&A...681A..79E*
DOI: 10.1051/0004-6361/202347932

TITLE: Magnetic field properties inside the jet of Mrk 421. Multiwavelength polarimetry, including the Imaging X-ray Polarimetry Explorer

AUTHOR: Kim, D. E., Di Gesu, L., Liodakis, I., Marscher, A. P., Jorstad, S. G., Middei, R., Marshall, H. L., Pacciani, L., Agudo, I., Tavecchio, F., Cibrario, N., Tugliani, S., Bonino, R., Negro, M., Puccetti, S., Tombesi, F., Costa, E., Donnarumma, I., Soffitta, P., Mizuno, T., Fukazawa, Y., Kawabata, K. S., Nakaoka, T., Uemura, M., Imazawa, R., Sasada, M., Akitaya, H., Josè Aceituno, F., Bonnoli, G., Casanova, V., Myserlis, I., Sievers, A., Angelakis, E., Kraus, A., Yeon Cheong, W., Jeong, H.-W., Kang, S., Kim, S.-H., Lee, S.-S., Agìs-Gonzàlez, B., Sota, A., Escudero, J., Gurwell, M., Keating, G. K., Rao, R., Kouch, P. M., Lindfors, E., Bourbah, I. G., Kiehlmann, S., Kontopodis, E., Mandarakas, N., Romanopoulos, S., Skalidis, R., Vervelaki, A., Savchenko, S. S., Antonelli, L. A., Bachetti, M., Baldini, L., Baumgartner, W. H., Bellazzini, R., Bianchi, S., Bongiorno, S. D., Brez, A., Bucciantini, N., Capitanio, F., Castellano, S., Cavazzuti, E., Chen, C.-T., Ciprini, S., De Rosa, A., Del Monte, E., Di Lalla, N., Di Marco, A., Doroshenko, V., Dovčiak, M., Ehlert, S. R., Enoto, T., Evangelista, Y., Fabiani, S., Ferrazzoli, R., Garcia, J. A., Gunji, S., Hayashida, K., Heyl, J., Iwakiri, W., Kaaret, P., Karas, V., Kislat, F., Kitaguchi, T., Kolodziejczak, J. J., Krawczynski, H., La Monaca, F., Latronico, L., Maldera, S., Manfreda, A., Marin, F., Marinucci, A., Massaro, F., Matt, G., Mitsuishi, I., Muleri, F., Ng, C.-Y., O'Dell, S. L., Omodei, N., Oppedisano, C., Papitto, A., Pavlov, G. G., Peirson, A. L., Perri, M., Pesce-Rollins, M., Petrucci, P.-O., Pilia, M., Possenti, A., Poutanen, J., Ramsey, B. D., Rankin, J., Ratheesh, A., Roberts, O., Romani, R. W., Sgró, C., Slane, P., Spandre, G., Swartz, D., Tamagawa, T., Taverna, R., Tawara, Y., Tennant, A. F., Thomas, N. E., Trois, A., Tsygankov, S. S., Turolla, R., Vink, J., Weisskopf, M. C., Wu, K., Xie, F., Zane, S.

PUBLICATION: *Astronomy and Astrophysics, 681, A12*

PUBLICATION DATE: 01/2024

ABSTRACT: *https://ui.adsabs.harvard.edu/abs/2024A&A...681A..12K*

DOI: 10.1051/0004-6361/202347408

Photo by Brooks Rownd

The Submillimeter Array (SMA) is a pioneering radio-interferometer dedicated to a broad range of astronomical studies including finding protostellar disks and outflows; evolved stars; the Galactic Center and AGN; normal and luminous galaxies; and the solar system. Located on Maunakea, Hawaii, the SMA is a collaboration between the Smithsonian Astrophysical Observatory and the Academia Sinica Institute of Astronomy and Astrophysics.

SUBMILLIMETER ARRAY
Center for Astrophysics | Harvard & Smithsonian
60 Garden Street, MS 78
Cambridge, MA 02138 USA
www.cfa.harvard.edu/sma/

SMA HILO OFFICE
645 North A'ohoku Place
Hilo, Hawaii 96720
Ph. 808.961.2920
Fx. 808.961.2921
sma1.sma.hawaii.edu

ACADEMIA SINICA INSTITUTE
OF ASTRONOMY & ASTROPHYSICS
11F of Astronomy-Mathematics Building,
AS/NTU, No. 1, Sec. 4, Roosevelt Road
Taipei 10617
Taiwan R.O.C.
www.asiaa.sinica.edu.tw/